


Locating sources of Szegedy's quantum network

Hong-Jue Wang ^{1,*}, Zhao-Long Hu,² Shu-Yu Shao,³ Fang-Feng Zhang,⁴ and Li Tao⁴

¹*School of Information Beijing Wuzi University, 101149 Beijing, People's Republic of China*

²*College of Mathematics and Computer Science Zhejiang Normal University, 321004 Jinhua, People's Republic of China*

³*Logistics School, Beijing Wuzi University, 101149 Beijing, People's Republic of China*

⁴*School of Statistics and Data Science, Beijing Wuzi University, 101149 Beijing, People's Republic of China*



(Received 27 January 2023; accepted 6 December 2023; published 25 January 2024)

Source location in quantum networks is a critical area of research with profound implications for cutting-edge fields such as quantum state tomography, quantum computing, and quantum communication. In this study, we present groundbreaking research on the technique and theory of source location in Szegedy's quantum networks. We develop a linear system evolution model for a Szegedy's quantum network system using matrix vectorization techniques. Subsequently, we propose a highly precise and robust source-location algorithm based on compressed sensing specifically tailored for Szegedy's quantum network. To validate the effectiveness and feasibility of our algorithm, we conduct numerical simulations on various model and real networks, yielding compelling results. These findings underscore the potential of our approach in practical applications.

DOI: [10.1103/PhysRevE.109.014311](https://doi.org/10.1103/PhysRevE.109.014311)

I. INTRODUCTION

Research on quantum networks based on quantum walk has gained significant attention in recent years due to advancements in quantum communication and quantum computation [1]. Within this domain, the task of locating the source nodes of a quantum message through partial observations of a quantum network is referred to as quantum network source location. Alternatively, from a system control perspective, quantum network source location can be viewed as inferring the initial state of a quantum network system based on limited observational information.

Quantum state tomography, a crucial area of study in quantum information, aims to infer the input quantum states by analyzing the output information of a quantum system [2]. This field is closely related to quantum network source location. However, most existing methods for quantum state tomography do not incorporate quantum walks for modeling and analysis. To address this gap, we propose a theoretical model called quantum network source location, which introduces new concepts for the development of precise and robust quantum state tomography methods. Quantum network source location holds significant potential in quantum computing, specifically in the transfer of quantum messages through reversible quantum logic gates [3]. Prior to conducting quantum computations, it is essential to prepare high-quality superposed quantum states [4], as the quality of these states directly impacts the accuracy and effectiveness of computational measurements. To ensure the quality of superposed states, we can employ quantum network source-location techniques by creating a quantum network system evolution model and performing source-location operations. Additionally, quantum network source location can be utilized for tracking the origin

of quantum messages and detecting cascade failures within quantum networks.

The concept of discrete quantum walk was first introduced by Aharonov *et al.* [5]. In this paradigm, the Hilbert space comprises the position space and the coin space, where the former corresponds to network nodes and the latter controls the walk direction. Quantum walks exhibit distinctive properties, attributed to coherence, that set them apart from classical random walks. These properties include high operational efficiency, absence of steady state, and nonuniform probability distribution. Over time, researchers have proposed various types of discrete quantum walks tailored to networks with diverse topologies and applications. These include coin quantum walk [6], Szegedy's quantum walk [7,8], and scattering quantum walk [9,10]. Coin quantum walk operates on one-dimensional lines or regular networks, while Szegedy's quantum walk accommodates arbitrary high-dimensional heterogeneous networks. Scattering quantum walk, on the other hand, is primarily suited for regular networks in which the position space corresponds to connected edges, obviating the need for an additional coin space. Lovett *et al.* [6] demonstrated that coin quantum walk can be leveraged to construct universal quantum logic gates, offering theoretical support for quantum computer design and algorithm development. Paparo *et al.* [8] proposed a quantum PageRank metric utilizing Szegedy's quantum walk results to measure the centrality of network nodes. This algorithm exploits the superposition of quantum walker states, significantly enhancing centrality computation speed. Yanmei Liu *et al.* [9] devised an efficient search algorithm for star networks using scattering quantum walk, achieving search accuracy of over 92.9% for specific connected edges. Titchener *et al.* [11] investigated the physical implementation of quantum walk by modeling it with the evolution of entangled photon pairs in coupled waveguides. They also proposed a method to vectorize the density matrix of quantum systems, enabling the reconstruction of initial photon states. Rhodes *et al.* [12] proposed a quantum walk search

*wanghongjue@bwu.edu.cn

algorithm on fully bipartite networks based on coin quantum walk, incorporating both nodes and connected edges as state spaces. Martín-Vázquez *et al.* [13] introduced a time-varying discrete quantum walk, identifying the sequence of coin operators that maximizes network transmission efficiency.

The study of source location in conventional message propagation on complex networks has made significant advancements over the past decade [14]. Researchers have delved deeper into this subject due to its complexity and diverse practical requirements [15,16]. The focus of research has shifted from single-source locations to multisource scenarios [17–20]. Additionally, there has been a transition from studying tree-structured network source location to examining general networks with complex topology [21,22], as well as a move away from specific propagation models towards developing universal algorithms suitable for various propagation models [23,24]. However, existing research has primarily focused on classical message propagation models, with limited exploration of quantum messages involving entangled states, superposed states, unmeasurable values, and other properties. Nonetheless, the successful outcomes of classical message source-location algorithms for complex networks provide valuable insights. While applying these algorithms directly to source location in quantum networks is challenging, lessons learned from investigating the accuracy of source location in complex networks can inspire further research. First, the scope of complex network source-location research can be extended to encompass quantum networks, including the study of source location in different model networks, optimizing the efficiency of source-location accuracy algorithms, and addressing challenges related to multisource location. Second, [25] consider the accuracy of complex network source location as a reconstruction problem concerning the initial state of linear systems and propose a source-location algorithm based on compressed sensing. Quantum information within quantum networks also exhibits sparsity properties at the initial time. Therefore, if a linear evolution model for quantum network systems can be established, the theory of compressed sensing is well-suited to address the source-location problem in quantum networks.

There exists a significant research gap concerning the fundamental correlation between classical complex network source location and quantum network source location [26]. Furthermore, there is a lack of effective algorithms and theories for accurately locating sources in quantum networks. This paper aims to address these issues by undertaking an analysis of the evolution mechanism of Szegedy's quantum walk. We reduce the Szegedy's quantum walk model and establish a linear Szegedy's quantum network system with observable information using the matrix vectorization technique [11]. To enhance algorithm efficiency, we approximate and simplify the linear evolution model, ultimately employing the theory of compressed sensing to solve the source-location problem in the Szegedy's quantum network.

The rest of this paper is structured as follows: In Sec. 2, we introduce the concept of Szegedy's quantum network and present two crucial theorems for reducing the original Szegedy's quantum network. In Sec. 3, we establish a linear evolution model of the Szegedy's quantum network system and propose a source-location model. With a focus on

algorithm efficiency, in Sec. 4, we simplify the Szegedy's quantum network source model in a reasonable manner and proposed a source-location algorithm based on the compressive sensing theory. Subsequently, in Sec. 5, we conduct simulations and verify the effectiveness of the proposed source-location algorithm on both model and real networks. Finally, we conclude the paper in Sec. 6.

II. SZEGEDY'S QUANTUM NETWORK

Here is a connected undirected network $G = (V, E)$ without self-loops, where $|V| = N$ is the number of nodes and $|E| = M$ is the number of edges in the network. G can be represented by a symmetric adjacency matrix A , element $a_{i,j}$ in A represents the connection of nodes v_i and v_j . If $a_{i,j} = 1$, there is a link between nodes v_i and v_j , that is to say, nodes v_i and v_j are neighbors to each other. For convenience, we refer to $a_{i,j}$ as the directed edge from node v_i to v_j , and $a_{j,i}$ as the directed edge from node v_j to v_i . For an undirected network G , $a_{i,j} = a_{j,i}$. $a_{i,j} = 0$ represents that nodes v_i and v_j are not connected. In a classical random walk, a walker can only locate at node v_i in the network at some time and move to a neighbor node of v_i with a certain probability at the next unit time. The state space of a walker in a classical random walk can be expressed as an N -dimensional vector space H^C , and the computational basis states of H^C are

$$|v_1\rangle = \begin{pmatrix} 1 \\ 0 \\ 0 \\ \vdots \\ 0 \end{pmatrix}, \quad |v_2\rangle = \begin{pmatrix} 0 \\ 1 \\ 0 \\ \vdots \\ 0 \end{pmatrix}, \quad \dots, \quad |v_N\rangle = \begin{pmatrix} 0 \\ 0 \\ 0 \\ \vdots \\ N \end{pmatrix},$$

where $|\cdot\rangle$ is the Dirac symbol and represents a state vector. Then the definition of Szegedy's quantum network is given below. First, $H = \text{span}\{|v_i, v_j\rangle, v_i, v_j \in V\}$ is defined as the Hilbert space spanned by the directed edges of network G , where $|v_i, v_j\rangle = |v_i\rangle \otimes |v_j\rangle$, so the dimension of space H is N^2 . In fact, each edge in the undirected network G is treated as two directed edges. Then, define the vector

$$|\psi_i\rangle = |v_i\rangle \otimes \sum_{j=1}^N \sqrt{\frac{a_{i,j}}{\sum_{j=1}^N a_{i,j}}} |v_j\rangle. \quad (1)$$

Here the vector $|\psi_i\rangle$ is superposition state of all directed edges from node v_i , and obviously all vectors $|\psi_i\rangle$ ($i = 1, 2, \dots, N$) are normalized. Because G is a connected undirected network without self-loops, the vector $|\psi_i\rangle$ can also be expressed as

$$|\psi_i\rangle = \frac{1}{\sqrt{k_i}} |v_i\rangle \otimes \sum_{j=1}^N a_{i,j} |v_j\rangle, \quad (2)$$

where k_i is the degree of the node v_i . The elements 0 in the vector $|\psi_i\rangle$ represent nonexistent self-loops and directed edges. In this paper, the initial state of Szegedy's quantum network system at time 0 is

$$|\psi(0)\rangle = \sum_{i=1}^N \alpha_i |\psi_i\rangle, \quad (3)$$

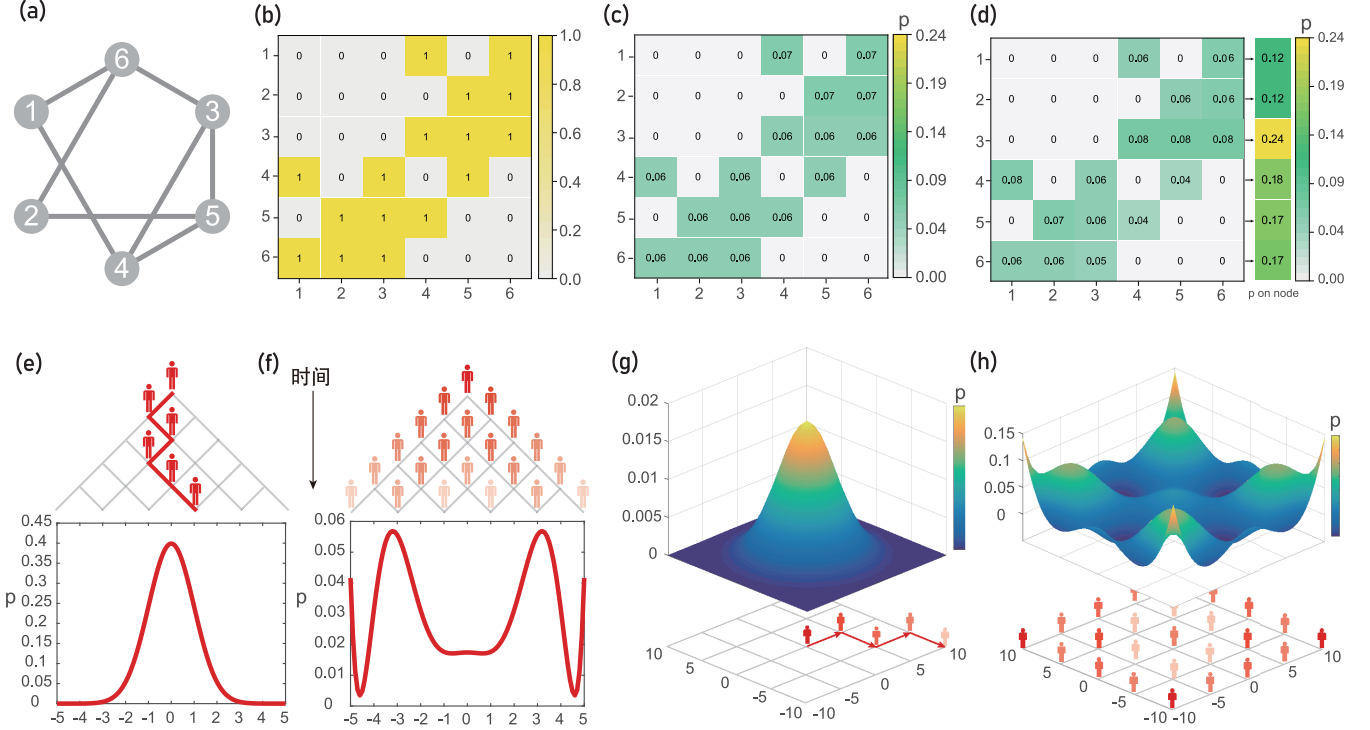


FIG. 1. Comparison between a classical random walk and a quantum walk. (a) A simple network with six nodes. Numbers in the center of nodes are the serial numbers of nodes. (b) The heat map of the network adjacency matrix A in panel (a). (c) The probability that the walker locates at each directed edge after Szegedy's quantum walk on the network in panel (a). (d) The result of converting the probability that the quantum walker locates at edges in (c) to nodes. (e) A classical random walk on a one-dimensional line. (f) Szegedy's quantum walk on a one-dimensional line. (g), (h) The probability distributions of a classical random walk and Szegedy's quantum walk on a two-dimensional grid, respectively.

where the complex number α_i satisfy the normalization condition $\sum_{i=1}^N |\alpha_i|^2 = |\langle \psi(0) | \psi(0) \rangle| = 1$, and $\langle \cdot |$ represents the conjugate transpose of the state vector $|\cdot\rangle$. $\langle \alpha | \beta \rangle$ represents the inner product of two vectors $\langle \alpha |$ and $|\beta\rangle$. If we observe state $|\psi(0)\rangle$ of a quantum walker, we find that the quantum walker locates at states $|\psi_i\rangle$ ($i = 1, 2, \dots, N$) with probability $P(0) = [|\alpha_1|^2 |\alpha_2|^2 \dots |\alpha_N|^2]^T$. $|\psi(0)\rangle$ is the superposition state of vectors $|\psi_i\rangle$ ($i = 1, 2, \dots, N$), which is also known as the wave function of the quantum system.

Szegedy's quantum network system is controlled by an $N^2 \times N^2$ unitary transformation matrix U , and the system state at time t can be expressed as

$$|\psi(t)\rangle = U |\psi(t-1)\rangle, \quad (4)$$

where $|\langle \psi(t) | \psi(t) \rangle| = |\langle \psi(t-1) | U^\dagger U | \psi(t-1) \rangle| = |\langle \psi(t-1) | \psi(t-1) \rangle| = 1$; that is, U can maintain the normalization condition of the system. Obviously, $|\psi(t)\rangle = U^t |\psi(0)\rangle$. The unitary transformation matrix U of Szegedy's quantum network system is

$$U = S(2\Pi - I), \quad (5)$$

where $S = \sum_{i,j=1}^N |v_i, v_j\rangle \langle v_j, v_i|$ is shift operator, $\Pi = \sum_{i=1}^N |\psi_i\rangle \langle \psi_i|$, $|\alpha\rangle \langle \beta|$ represents outer product of two vectors, and I is identity matrix. Clearly, S and Π are both symmetric matrices.

According to the definition of Szegedy's quantum walk, the walker is located in the superposition state of the

directed edges of the network. Actually, we can convert the probability of the quantum walker to locate at directed edges into the probability of the walker locate at nodes; that is, the probability of the walker locate at node v_i is the sum of the probabilities of the walker locate at the directed edges starting from node v_i . Figure 1 is a schematic diagram of converting probability of quantum walker locate at directed edges to nodes and comparison between the classical random walk and the Szegedy's quantum walk. Figure 1(a) shows a simple network with six nodes. Numbers in the center of nodes are the serial numbers of nodes. Figure 1(b) is the heat map of the network adjacency matrix A in Fig. 1(a). Each element in the matrix corresponds to an edge of the network, and $a_{i,j} = 1$ represents the existence of an edge and $a_{i,j} = 0$ otherwise. Figure 1(c) is the probability that the walker locate at each directed edge after the Szegedy's quantum walk on the network in Fig. 1(a). Figure 1(d) is the result of converting the probability that the quantum walker locate at edges in Fig. 1(c) to nodes. The probability that the quantum walker locate at node v_i is obtained by summing the values of row i of the matrix in Fig. 1(c). Figure 1(e) is a classical random walk on a one-dimensional line. A random walker starts from the initial coordinate zero. The walker can only move to the left or right at each time step with probability of 0.5. After enough time, the probability of the walker to be given coordinate on the line obeys a Gaussian distribution. Figure 1(f) is Szegedy's quantum walk on a one-dimensional line. The walker starts the quantum walk from coordinate zero, that

is, at the initial time, the quantum walker is located at the superposition state of the left and right edges which connect to coordinate zero, and the moving direction chosen by the quantum walker at each time step is the superposition state of the left and right directions. After enough time, the probability of the quantum walker to be located at different coordinates on the line follows a non-Gaussian distribution. Figures 1(g) and 1(h) are the probability distributions of classical random walk and Szegedy's quantum walk on a two-dimensional grid, respectively. According to the central limit theorem, the probability of a classical random walker locate at each node after evolution obeys a two-dimensional Gaussian distribution [27], while Szegedy's quantum walk obeys a non-Gaussian distribution.

It is worth pointing out that another way to describe the state of a quantum system is using the density matrix, which is defined as

$$\rho(t) = |\psi(t)\rangle\langle\psi(t)|. \quad (6)$$

The main diagonal element of the density matrix represents the probability of the quantum walker to be located at each directed edge of the network, which corresponds to the elements in $\mathbf{P}(t)$. Therefore, the trace of the density matrix $\rho(t)$ is one. As the density matrix can describe all measurable information of the quantum system, it is equivalent to the wave function $|\psi(t)\rangle$. Hence, we can also use the density matrix to describe the state of Szegedy's quantum walker on networks. Then the evolution equation of the Szegedy's quantum network system can also be

$$\rho(t+1) = U\rho(t)U^T. \quad (7)$$

Obviously, $\rho(t) = U^t\rho(0)(U^T)^t$.

Here we give two theorems of Szegedy's quantum walk on complex networks.

Theorem 1. Let matrix $\psi = [|\psi_1\rangle|\psi_2\rangle\cdots|\psi_N\rangle]$ with dimension $N^2 \times N$ be composed of all vectors $|\psi_i\rangle$ ($i = 1, 2, \dots, N$) of Szegedy's quantum walk. For the initial state $|\psi(0)\rangle = \sum_{i=1}^N \alpha_i |\psi_i\rangle$, the positions of rows with all zeros in matrix ψ are the same as in vector $U^t|\psi(0)\rangle$, where the variable t is an arbitrary positive integer.

Proof. In fact, when nodes v_i and v_j are not connected, $a_{i,j} = 0$, which leads to some vectors of $a_{i,j}|v_i, v_j\rangle$ ($i, j = 1, 2, \dots, N$) having the same locations of the value zero. Since $|\psi_i\rangle = \sum_{j=1}^N \frac{a_{i,j}}{\sqrt{k_i}} |v_i, v_j\rangle$ ($i = 1, 2, \dots, N$), the positions where the elements are zero in $a_{i,j}|v_i, v_j\rangle$ ($i, j = 1, 2, \dots, N$) are also zero in $|\psi_i\rangle$ ($i = 1, 2, \dots, N$). Furthermore, since $\psi = [|\psi_1\rangle|\psi_2\rangle\cdots|\psi_N\rangle]$, it follows that the corresponding rows in ψ are all zero. Clearly, due to the fact that $\frac{1}{\sqrt{k_i}} > 0$ ($i = 1, 2, \dots, N$) in the connected network, the positions where $a_{i,j}|v_i, v_j\rangle$ ($i = 1, 2, \dots, N$) are simultaneously zero correspond one to one with the rows in ψ that are also zero. Therefore, to prove Theorem 1, it suffices to show that the positions where $a_{i,j}|v_i, v_j\rangle$ ($i = 1, 2, \dots, N$) are simultaneously zero in the vector $U^t|\psi(0)\rangle$ are also zero. Since $|\psi(0)\rangle = \sum_{i=1}^N \alpha_i |\psi_i\rangle = \sum_{i,j=1}^N \frac{\alpha_i a_{i,j}}{\sqrt{k_i}} |v_i, v_j\rangle$, it follows that $U^t|\psi(0)\rangle = \sum_{i=1}^N \alpha_i U^t|\psi_i\rangle = \sum_{i,j=1}^N \frac{\alpha_i}{\sqrt{k_i}} U^t(a_{i,j}|v_i, v_j\rangle)$. Therefore, to demonstrate that the positions where $a_{i,j}|v_i, v_j\rangle$ ($i, j = 1, 2, \dots, N$) are simultaneously zero in the vector $U^t|\psi(0)\rangle$, we only need to establish that the positions where $a_{i,j}|v_i, v_j\rangle$ ($i = 1, 2, \dots, N$) are simultaneously zero in $U^t(a_{i,j}|v_i, v_j\rangle)$ are zero. We start by examining the case of $U(a_{i,j}|v_i, v_j\rangle)$:

$$\begin{aligned} U(a_{i,j}|v_i, v_j\rangle) &= a_{i,j} \left(\sum_{m,n=1}^N |v_m, v_n\rangle\langle v_n, v_m| \right) \left(2 \sum_{x,y=1}^N \frac{a_{1,x}a_{1,y}}{k_1} |v_1, v_x\rangle\langle v_1, v_y| + \cdots \right. \\ &\quad \left. + 2 \sum_{x,y=1}^N \frac{a_{i,x}a_{i,y}}{k_i} |v_i, v_x\rangle\langle v_i, v_y| + \cdots + 2 \sum_{x,y=1}^N \frac{a_{N,x}a_{N,y}}{k_N} |v_N, v_x\rangle\langle v_N, v_y| - I |v_i, v_j\rangle \right) \\ &= a_{i,j} \left(\sum_{m,n=1}^N |v_m, v_n\rangle\langle v_n, v_m| \right) \left(2 \sum_{x,y=1}^N \frac{a_{1,x}a_{1,y}}{k_1} |v_1, v_x\rangle\langle v_1, v_y| + \cdots \right. \\ &\quad \left. + 2 \sum_{x,y=1}^N \frac{a_{i,x}a_{i,y}}{k_i} |v_i, v_x\rangle\langle v_i, v_y| + \cdots \right. \\ &\quad \left. + 2 \sum_{x,y=1}^N \frac{a_{N,x}a_{N,y}}{k_N} |v_N, v_x\rangle\langle v_N, v_y| - |v_i, v_j\rangle \right). \end{aligned}$$

For $2 \sum_{x,y=1}^N \frac{a_{h,x}a_{h,y}}{k_h} |v_h, v_x\rangle\langle v_h, v_y|$, only when $h = i, y = j$, $\langle v_h, v_y|v_i, v_j\rangle = 1$, and for other cases, $\langle v_h, v_y|v_i, v_j\rangle = 0$. Thus, we obtain

$$2 \sum_{x,y=1}^N \frac{a_{h,x}a_{h,y}}{k_h} |v_h, v_x\rangle\langle v_h, v_y|v_i, v_j\rangle = 2 \sum_{x=1}^N \frac{a_{i,x}a_{i,j}}{k_i} |v_i, v_x\rangle.$$

Therefore, the original expression is

$$\begin{aligned}
 & a_{i,j} \left(\sum_{m,n=1}^N |v_m, v_n\rangle \langle v_n, v_m| \right) \left(2 \sum_{x=1}^N \frac{a_{i,x} a_{i,j}}{k_i} |v_i, v_x\rangle - |v_i, v_j\rangle \right) \\
 &= a_{i,j} \left(\sum_{m,n=1}^N |v_m, v_n\rangle \langle v_n, v_m| \right) \left(\frac{2a_{i,1} a_{i,j}}{k_i} |v_i, v_1\rangle + \dots + \frac{2a_{i,j} a_{i,j}}{k_i} |v_i, v_j\rangle + \dots + \frac{2a_{i,N} a_{i,j}}{k_i} |v_i, v_N\rangle - |v_i, v_j\rangle \right) \\
 &= \frac{2a_{i,1} a_{i,j}}{k_i} \sum_{m,n=1}^N |v_m, v_n\rangle \langle v_n, v_m |v_i, v_1\rangle + \dots + \frac{2a_{i,j} a_{i,j}}{k_i} \sum_{m,n=1}^N |v_m, v_n\rangle \langle v_n, v_m |v_i, v_j\rangle + \dots \\
 &\quad + \frac{2a_{i,N} a_{i,j}}{k_i} \sum_{m,n=1}^N |v_m, v_n\rangle \langle v_n, v_m |v_i, v_N\rangle - a_{i,j} \sum_{m,n=1}^N |v_m, v_n\rangle \langle v_n, v_m |v_i, v_j\rangle.
 \end{aligned}$$

For $\sum_{m,n=1}^N |v_m, v_n\rangle \langle v_n, v_m |v_i, v_h\rangle$, where $n = i, m = h$, we have $\langle v_n, v_m |v_i, v_h\rangle = 1$, for other cases, it is zero, therefore, we obtain $\sum_{m,n=1}^N |v_m, v_n\rangle \langle v_n, v_m |v_i, v_h\rangle = |v_h, v_i\rangle$. Thus, the original expression is

$$\begin{aligned}
 & \frac{2a_{i,1} a_{i,j}}{k_i} |v_1, v_i\rangle + \dots + \frac{2a_{i,j} a_{i,j}}{k_i} |v_j, v_i\rangle + \dots + \frac{2a_{i,N} a_{i,j}}{k_i} |v_N, v_i\rangle - a_{i,j} |v_j, v_i\rangle \\
 &= \sum_{m=1}^N \frac{2a_{i,m} a_{i,j}}{k_i} |v_m, v_i\rangle - a_{i,j} |v_j, v_i\rangle = \sum_{m=1}^N \frac{2a_{i,m}}{k_i} (a_{i,j} |v_m, v_i\rangle) - a_{i,j} |v_j, v_i\rangle.
 \end{aligned}$$

It can be seen that $U|v_i, v_j\rangle$ is a linear combination of $a_{i,j}|v_1, v_i\rangle, \dots, a_{i,j}|v_j, v_i\rangle, \dots, a_{i,j}|v_N, v_i\rangle$, and $a_{i,j}|v_1, v_j\rangle, \dots, a_{i,j}|v_j, v_j\rangle, \dots, a_{i,j}|v_N, v_j\rangle$ is a subset of all $a_{i,j}|v_i, v_j\rangle$ ($i = 1, 2, \dots, N$). Therefore, if all the positions of $a_{i,j}|v_i, v_j\rangle$ ($i = 1, 2, \dots, N$) being zero are also zero in $a_{i,j}|v_1, v_i\rangle, \dots, a_{i,j}|v_j, v_i\rangle, \dots, a_{i,j}|v_N, v_i\rangle$, then the corresponding positions of $U|v_i, v_j\rangle$ are also zero. From $U(a_{i,j}|v_i, v_j\rangle) = \sum_{m=1}^N \frac{2a_{i,m}}{k_i} (a_{i,j}|v_m, v_i\rangle) - a_{i,j}|v_j, v_i\rangle$ we know that $U^2(a_{i,j}|v_i, v_j\rangle) = \sum_{m=1}^N \frac{2a_{i,m}}{k_i} U(a_{i,j}|v_m, v_i\rangle) - U(a_{i,j}|v_j, v_i\rangle)$. Similarly, for $U(a_{i,j}|v_m, v_i\rangle)$ and $U(a_{i,j}|v_j, v_i\rangle)$ we can reach the same conclusion. That is, if all the positions of $a_{i,j}|v_i, v_j\rangle$ ($i = 1, 2, \dots, N$) being zero are also zero in $U(a_{i,j}|v_m, v_i\rangle)$ and $U(a_{i,j}|v_j, v_i\rangle)$, then they are also zero in $U^2(a_{i,j}|v_i, v_j\rangle)$. By induction, we know that all the positions of $a_{i,j}|v_i, v_j\rangle$ ($i, j = 1, 2, \dots, N$) being zero are also zero in $U^t(a_{i,j}|v_i, v_j\rangle)$. The proof is complete. ■

In fact, based on Theorem 1, we show in the following Theorem 2 that we can remove the rows with all zeros from matrix ψ and get a reduced Szegedy's quantum walk, along with the corresponding reduced vectors $|\psi_i\rangle$ ($i = 1, 2, \dots, N$) and reduced unitary matrix.

Suppose the elements in rows m_1, m_2, \dots, m_L of matrix ψ are not all zero. We define the reduction matrix C as the matrix obtained by taking out the elements in positions m_1, m_2, \dots, m_L of ψ , i.e., $C|\psi_i\rangle$ is a new vector $|\psi_i\rangle$ formed by extracting the elements at positions m_1, m_2, \dots, m_L from $|\psi_i\rangle$. Since $|\psi_i\rangle = \sum_{j=1}^N \frac{a_{i,j}}{\sqrt{k_i}} |v_i, v_j\rangle$, where $\frac{a_{i,j}}{\sqrt{k_i}} \geq 0$, all the elements at positions m_1, m_2, \dots, m_L in $|v_i, v_j\rangle$ ($i, j = 1, 2, \dots, N$) are also nonzero. Now, we remove the elements at positions m_1, m_2, \dots, m_L from all $|v_i, v_j\rangle$

($i, j = 1, 2, \dots, N$) to obtain new vectors $C|v_i, v_j\rangle$ ($i, j = 1, 2, \dots, N$). Obviously, the matrix C satisfies $CC^T = I$, where $C^T C$ is a diagonal matrix with ones at positions (m_i, m_i) ($i = 1, 2, \dots, L$) and zeros everywhere else. Thus, $C^T C \cdot d$ sets all the elements in vector d except those at positions m_1, m_2, \dots, m_L to zero, while keeping the values of elements at positions m_1, m_2, \dots, m_L unchanged. Therefore, from the properties of $a_{i,j}|v_i, v_j\rangle$ and $|\psi_i\rangle$, we have $C^T C a_{i,j}|v_i, v_j\rangle = a_{i,j}|v_i, v_j\rangle$, which implies $C^T C |\psi_i\rangle = |\psi_i\rangle$. Similarly, we have $a_{i,j}\langle v_i, v_j | C^T C = a_{i,j}\langle v_i, v_j |$ and $\langle \psi_i | C^T C = \langle \psi_i |$. Consequently, we obtain $C^T C \cdot \Pi = \Pi$, as well as $\Pi \cdot C^T C = \Pi$. Based on this, we establish the following theorem:

Theorem 2. When simplification operations are applied to ψ and $|v_i, v_j\rangle$, we obtain $C|v_i, v_j\rangle$ and $C|\psi_i\rangle$. Consequently, the matrices S , Π , and U transform into CSC^T , $C\Pi C^T$, and CUC^T , respectively. Moreover, the state $|\psi(t)\rangle = U^t \sum_{i=1}^N \alpha_i |\psi_i\rangle$ becomes $C \cdot |\psi(t)\rangle$.

Proof. For matrix $S = \sum_{i,j=1}^N |v_i, v_j\rangle \langle v_j, v_i|$, we have

$$\begin{aligned}
 \sum_{i,j=1}^N C|v_i, v_j\rangle \langle v_j, v_i| C^T &= C \left(\sum_{i,j=1}^N |v_i, v_j\rangle \langle v_j, v_i| \right) C^T \\
 &= CSC^T.
 \end{aligned}$$

For matrix $\Pi = \sum_{i=1}^N |\psi_i\rangle \langle \psi_i|$, we have $\sum_{i=1}^N C|\psi_i\rangle \langle \psi_i| C^T = C(\sum_{i=1}^N |\psi_i\rangle \langle \psi_i|) C^T = C\Pi C^T$. For matrix $U = S(2\Pi - I)$, we have $CSC^T(2C\Pi C^T - I) = 2CSC^T C\Pi C^T - CSC^T = 2C\Sigma\Pi C^T - CSC^T = CS(2\Pi - I)C^T = CUC^T$. For vector $|\psi(t)\rangle = U^t \sum_{i=1}^N \alpha_i |\psi_i\rangle$, according to Theorem 1, all elements in $U^t \sum_{i=1}^N \alpha_i |\psi_i\rangle$ except for positions m_1, m_2, \dots, m_L are zero. Also, by the action of $C^T C$, we know

that $C^T C U^t \sum_{i=1}^N \alpha_i |\psi_i\rangle = U^t \sum_{i=1}^N \alpha_i |\psi_i\rangle$, which means $C^T C |\psi(t)\rangle = |\psi(t)\rangle$. After performing the simplification operation, we obtain

$$\begin{aligned} & (CUC^T)^t C \sum_{i=1}^N \alpha_i |\psi_i\rangle \\ &= CUC^T \cdot CUC^T \cdot \dots \cdot CUC^T \cdot CUC^T C \sum_{i=1}^N \alpha_i |\psi_i\rangle \\ &= CUC^T \cdot CUC^T \cdot \dots \cdot CUC^T \cdot CU \sum_{i=1}^N \alpha_i |\psi_i\rangle \end{aligned}$$

$$\begin{aligned} &= CUC^T \cdot CUC^T \cdot \dots \cdot CUC^T \sum_{i=1}^N \alpha_i |\psi_i\rangle \\ &= \dots = CU^t \sum_{i=1}^N \alpha_i |\psi_i\rangle = C \cdot |\psi(t)\rangle. \end{aligned}$$

Thus, the proof complete. \blacksquare

We denote $\bar{U} = CUC^T$ as the evolution matrix matrix of reduced Szegedy's quantum walk, the wave function of the reduced Szegedy's quantum walk is $|\bar{\psi}(t)\rangle = C|\psi(t)\rangle$. Obviously, $\bar{U}|\bar{\psi}(t)\rangle = CUC^T \cdot C|\psi(t)\rangle = CU|\psi(t)\rangle = C|\psi(t+1)\rangle = |\bar{\psi}(t+1)\rangle$. We prove that \bar{U} satisfies unitarity. First, we have

$$\begin{aligned} \bar{U}\bar{U}^T &= CSC^T(2C\Pi C^T - I)(2C\Pi C^T - I)CSC^T \\ &= 4CSC^T C\Pi C^T C\Pi C^T CSC^T - 4CSC^T C\Pi C^T CSC^T + CSC^T CSC^T \\ &= 4C\Sigma\Pi^2 SC^T - 4C\Sigma\Pi SC^T + CSC^T CSC^T. \end{aligned}$$

Since $\Pi^2 = (\sum_{i=1}^N |\psi_i\rangle\langle\psi_i|)(\sum_{j=1}^N |\psi_j\rangle\langle\psi_j|) = \sum_{i=1}^N |\psi_i\rangle\langle\psi_i| = \Pi$, we have the original expression is $4C\Sigma\Pi SC^T - 4C\Sigma\Pi SC^T + CSC^T CSC^T = CSC^T CSC^T$. In fact, according to the definition of matrix C , we already know that the positions m_1, m_2, \dots, m_L where the row elements of C are one also satisfy the condition that they are not all zero in all $|v_i, v_j\rangle$. And, since $|v_i, v_j\rangle = |v_i\rangle \otimes |v_j\rangle$, the positions m_1, m_2, \dots, m_L correspond to the elements one in the vectorization $\tilde{A} = [a_{1,1} \ a_{2,1} \ \dots \ a_{N,1} \ a_{1,2} \ a_{2,2} \ \dots \ a_{N,N}]^T$ of the adjacency matrix A , i.e., the elements at positions m_1, m_2, \dots, m_L in \tilde{A} are one, while other elements are zero. Since $a_{i,j}$ takes values of one or zero representing whether nodes v_i and v_j are connected, according to the action of matrix C , we have $CSC^T = C(\sum_{i,j=1}^N |v_i, v_j\rangle\langle v_j, v_i|)C^T = C(a_{i,j} \sum_{i,j=1}^N |v_i, v_j\rangle\langle v_j, v_i|)C^T$. So we have

$$\begin{aligned} CSC^T &= C \left(\sum_{i,j=1}^N |v_i, v_j\rangle\langle v_j, v_i| \right) C^T C \left(\sum_{m,n=1}^N |v_n, v_m\rangle\langle v_m, v_n| \right) C^T \\ &= C \left(a_{i,j} \sum_{i,j=1}^N |v_i, v_j\rangle\langle v_j, v_i| \right) C^T C \left(\sum_{m,n=1}^N a_{m,n} |v_n, v_m\rangle\langle v_m, v_n| \right) C^T \\ &= C \left(a_{i,j} \sum_{i,j=1}^N |v_i, v_j\rangle\langle v_j, v_i| \right) \left(\sum_{m,n=1}^N a_{m,n} |v_n, v_m\rangle\langle v_m, v_n| \right) C^T \\ &= C \left(a_{i,j} a_{m,n} \sum_{i,j,m,n=1}^N |v_i, v_j\rangle\langle v_j, v_i| |v_n, v_m\rangle\langle v_m, v_n| \right) C^T \\ &= C \left(a_{i,j} \sum_{i,j=1}^N |v_i, v_j\rangle\langle v_i, v_j| \right) C^T \\ &= C \left(\sum_{i,j=1}^N |v_i, v_j\rangle\langle v_i, v_j| \right) C^T = CC^T = I. \end{aligned}$$

That is, $\bar{U}\bar{U}^T = I$ and \bar{U} satisfies the unitary property. The proof is complete. \blacksquare

The density matrix corresponding to the reduced Szegedy's quantum walk is $\bar{\rho} = |\bar{\psi}\rangle\langle\bar{\psi}|$, and which satisfies $\bar{\rho}(t+1) = \bar{U}\bar{\rho}(t)\bar{U}^{-1}$ and $\bar{\rho}(t) = \bar{U}^t \bar{\rho}(0) (\bar{U}^{-1})^t$. Obviously, the reduced Szegedy's quantum network system is equivalent to the

original system. Figure 2 shows a schematic diagram of reducing the original Szegedy's quantum network system based on Theorems 1 and 2. Figure 2(a) shows a simple connected undirected network with three nodes and no self-loops. Numbers in the center of nodes are the serial numbers of nodes, v_1 (red), v_2 (green), and v_3 (blue). The connection of the

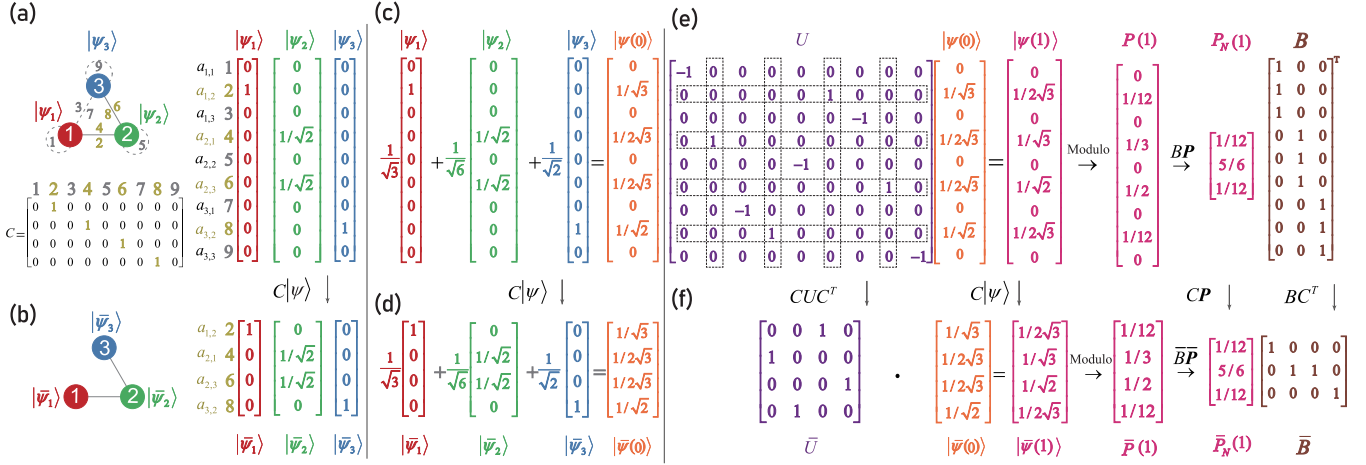


FIG. 2. Schematic diagram of reduction matrix C . (a) A simple of a connected undirected network with three nodes and without self-loops. (b) The result of removing the nonexistent directed edges and self-loops of networks in panel (a). (c) The quantum walk state vector $|\psi(0)\rangle$ at initial time 0. (d) $|\bar{\psi}(0)\rangle = C|\psi(0)\rangle$ which is obtained by the operation of the reduction matrix C . (e) $|\psi(1)\rangle$ after the evolution of the unitary matrix U on $|\psi(0)\rangle$ in panel (c). (f) The reduced matrix of U , probability P , and matrix B in panel (e).

network is $a_{1,2} = 1$ and $a_{2,3} = 1$. When Szegedy's quantum walk executes on the network, the network is regarded as a directed network, and the numbers near the network edges are the serial numbers of directed edges and self-loops. The real edges are existing, and the dashed edges are nonexistent. It can be seen that the directed edges existing in the network are $a_{1,2}$, $a_{2,1}$, $a_{2,3}$, and $a_{3,2}$, and their serial numbers are 2, 4, 6, 8, respectively. The dashed edges $a_{1,1}$, $a_{1,3}$, $a_{2,2}$, $a_{3,1}$, and $a_{3,3}$ are numbered 1, 3, 5, 7, and 9, respectively, which are nonexistent. The three nodes in the network correspond to three vectors $|\psi_1\rangle$ (red), $|\psi_2\rangle$ (green), and $|\psi_3\rangle$ (blue) of Szegedy's quantum network system. It can be seen that the first, third, fifth, seventh, and ninth elements of the three vectors $|\psi_1\rangle$, $|\psi_2\rangle$, and $|\psi_3\rangle$ are all zero, which corresponding to the nonexistent directed edges and self-loops $a_{1,1}$, $a_{1,3}$, $a_{2,2}$, $a_{3,1}$, and $a_{3,3}$ in the network. C is the reduction matrix. Since the elements at positions 2, 4, 6, and 8 in $|\psi_1\rangle$, $|\psi_2\rangle$, and $|\psi_3\rangle$ are not zero simultaneously, reduction matrix C has dimension 4×9 , and there is only one element of value one in each row of C which corresponding to the position of a nonzero element in vectors $|\psi_1\rangle$, $|\psi_2\rangle$, and $|\psi_3\rangle$; all the other elements of each row are zero. Figure 2(b) is the result of removing the nonexistent directed edges and self-loops of network in Fig. 2(a). After the action of reduction matrix C , new reduced vectors are $|\bar{\psi}_1\rangle = C|\psi_1\rangle$, $|\bar{\psi}_2\rangle = C|\psi_2\rangle$, and $|\bar{\psi}_3\rangle = C|\psi_3\rangle$ is obtained. Figure 2(c) shows the quantum walk state vector $|\psi(0)\rangle$ at initial time 0, and $|\psi(0)\rangle$ is represented linearly by the vectors $|\psi_1\rangle$, $|\psi_2\rangle$, and $|\psi_3\rangle$. Figure 2(d) is $|\bar{\psi}(0)\rangle = C|\psi(0)\rangle$ which obtained by the operation of reduction matrix C , $|\bar{\psi}(0)\rangle$ can be represented linearly by the new vectors $|\bar{\psi}_1\rangle$, $|\bar{\psi}_2\rangle$, and $|\bar{\psi}_3\rangle$, and the amplitudes are the same as in Fig. 2(c). Figure 2(e) is $|\psi(1)\rangle$ after the evolution of the unitary matrix U on $|\psi(0)\rangle$ in Fig. 2(c). It can be seen that rows 2, 4, 6, 8 and columns 2, 4, 6, 8 of the unitary matrix C have nonzero elements 1, which corresponds to the position of the nonzero element in vectors $|\psi_1\rangle$, $|\psi_2\rangle$, and $|\psi_3\rangle$, the position of the $|\psi(1)\rangle$ is also nonzero. All elements -1 exists in rows 1, 3, 5, 7, 9 and columns 1, 3, 5, 7, 9 of U correspond to the nonexistent directed edges and self-loops in the network, and also

correspond to the positions of simultaneous zeros in vectors $|\psi_1\rangle$, $|\psi_2\rangle$, and $|\psi_3\rangle$, the corresponding positions of $|\psi(1)\rangle$ are also zero. $P(1)$ is the probability of quantum walker located at each directed edge, and which is obtained by taking the modulus of the elements in $|\psi(1)\rangle$. $P(1)$ is an observable value, and $P_N(1) = BP(1)$ is the result of converting the probability of the quantum walker located at the edges of nodes. The dimensions of matrix B are $N \times N^2$, because each node is connected by at most three directed edges including self-loops, so each row of B has three elements as one, and in the i th row of B , the elements at positions $(i-1)N+1$, $(i-1)N+2$, \dots , iN are one, other elements are zero. Figure 2(f) is the reduced matrix of U , probability P , and matrix B in Fig. 2(e). It can be seen that $\bar{U} = CUC^T$ is the result after removing the rows and columns in U that correspond to nonexistent directed edges in the network. $\bar{P}(1) = CP(1)$ is given by removing elements zero from $P(1)$. After converting the probabilities $\bar{P}(1)$ on the edges to the nodes, it becomes $\bar{P}_N(1) = \bar{B}\bar{P}(1)$. Where $\bar{B} = BC^T$.

III. SZEGEDY'S QUANTUM NETWORK SOURCE-LOCATION MODEL BASED ON COMPRESSED SENSING THEORY

Szegedy's quantum network source location is actually to infer the position of nonzero elements in the initial state $|\bar{\psi}(0)\rangle$ of the quantum walker by using probabilities of the quantum walker locating at a fraction of nodes for some time steps. That is to say, based on partial observable information from $|\bar{\psi}(t)\rangle$ or $\bar{P}(t)$ at time t , we can infer the positions of non-zero elements in $|\bar{\psi}(0)\rangle$ or $\bar{P}(0)$. It can be seen from the equations $|\bar{\psi}(t)\rangle = \bar{U}(t)|\bar{\psi}(0)\rangle$ and $\bar{\rho}(t) = \bar{U}^t \bar{\rho}(0) (\bar{U}^{-1})^t$ that $|\bar{\psi}(0)\rangle$ can be obtained by using $|\bar{\psi}(t)\rangle$ through a simple matrix calculation, namely, $|\bar{\psi}(0)\rangle = (\bar{U}(t))^{-1} |\bar{\psi}(t)\rangle$ or $\bar{\rho}(0) = (\bar{U}^{-1})^t \bar{\rho}(t) \bar{U}^t$. Finally, the position of nonzero elements of $|\bar{\psi}(0)\rangle$ or the main diagonal of $\bar{\rho}(0)$ can be used to determine the initial source node of Szegedy's quantum network. However, the amplitudes in $|\bar{\psi}(t)\rangle$ are unobservable, and there are also many unobservable elements in $\bar{\rho}(t)$, which

reject the method of locating the sources of the quantum network by matrix computation. The only information we can obtain is the probability that the quantum walker located at each node, that is, $\bar{\rho}(t)$, which is the elements on the main diagonal of $\bar{\rho}(t)$. The physical realization of quantum walks contributes to a more detailed understanding of the evolution of quantum systems and facilitates the advancement of quantum computing research. The approach of utilizing the evolution process of photons in coupled waveguides for implementing quantum walks has garnered significant attention from researchers [28–30]. In the physical implementation of one-dimensional quantum walks, waveguides are placed in three-dimensional space, parallel to the y axis, with the x -axis coordinates corresponding to the waveguide labels. After releasing a photon at one end of the waveguide, the photon's position becomes entangled with different waveguides after a certain time evolution. At specific values of y , the photon can be detected with varying probabilities. By controlling the spacing between waveguides and the evolution time of the photon in the waveguide, the one-dimensional quantum walk can be controlled, and the distribution of photons can be observed [29]. The author elaborates on the detailed implementation of two-dimensional quantum walks using waveguides in Refs. [28,30]. Then, from a theoretical perspective, we establish a linear evolution model of the quantum network system by vectorizing the density matrix and propose the source-location model by compressed sensing theory which can provide theoretical and technical support for the physical implementation of quantum walks and quantum state tomography in arbitrary dimensions.

A. Linear Szegedy's quantum network system with observable values

First, we apply the following transformation to \bar{U} and $\bar{\rho}(t)$, respectively, in the equation $\bar{\rho}(t) = \bar{U}^t \bar{\rho}(0) (\bar{U}^t)^t$. That is, let

$$\tilde{U} = \bar{U} \otimes \bar{U}. \quad (8)$$

According to Theorem 2, the dimensions of \bar{U} are $L \times L$, and \bar{U}^\dagger is the conjugate matrix of \bar{U} , so the dimension of \tilde{U} is $L^2 \times L^2$. Then the density matrix $\bar{\rho}(t)$ with dimensions $L \times L$ is converted into a vector with dimensions $L^2 \times 1$ as

$$\tilde{\rho}(t) = \begin{bmatrix} \bar{\rho}_{1,1}(t) \\ \bar{\rho}_{2,1}(t) \\ \vdots \\ \bar{\rho}_{L,1}(t) \\ \bar{\rho}_{1,2}(t) \\ \bar{\rho}_{2,2}(t) \\ \vdots \\ \bar{\rho}_{L,L}(t) \end{bmatrix}, \quad (9)$$

where the $[k(L+1) - L]$ th element in $\tilde{\rho}(t)$ is the probability that the quantum walker is located at a directed edge; that is, the k th element on the main diagonal of the original $\bar{\rho}(t)$, where k is a positive integer. So the evolution equation of the reduced Szegedy's quantum network system turns out to be

$$\tilde{\rho}(t+1) = \tilde{U} \tilde{\rho}(t). \quad (10)$$

Let us prove Eq. (10). First, let us define

$$\bar{U} = \begin{bmatrix} \bar{U}_1 \\ \bar{U}_2 \\ \vdots \\ \bar{U}_L \end{bmatrix},$$

where $\bar{U}_i = [\bar{U}_{i,1} \bar{U}_{i,2} \cdots \bar{U}_{i,L}]$. Similarly, we define $\bar{\rho}(t) = [\bar{\rho}_1 \bar{\rho}_2 \cdots \bar{\rho}_L]$, where

$$\bar{\rho}_i = \begin{bmatrix} \bar{\rho}_{1,i} \\ \bar{\rho}_{2,i} \\ \vdots \\ \bar{\rho}_{L,i} \end{bmatrix}.$$

Then,

$$\begin{aligned} \bar{U} \bar{\rho}(t) \bar{U}^T &= \begin{bmatrix} \bar{U}_1 \\ \bar{U}_2 \\ \vdots \\ \bar{U}_L \end{bmatrix} \bar{\rho}(t) [\bar{U}_1^T \quad \bar{U}_2^T \quad \cdots \quad \bar{U}_L^T] \\ &= \begin{bmatrix} \bar{U}_1 \bar{\rho}(t) \bar{U}_1^T & \bar{U}_1 \bar{\rho}(t) \bar{U}_2^T & \cdots & \bar{U}_1 \bar{\rho}(t) \bar{U}_L^T \\ \bar{U}_2 \bar{\rho}(t) \bar{U}_1^T & \bar{U}_2 \bar{\rho}(t) \bar{U}_2^T & \cdots & \bar{U}_2 \bar{\rho}(t) \bar{U}_L^T \\ \vdots & \vdots & \vdots & \vdots \\ \bar{U}_L \bar{\rho}(t) \bar{U}_1^T & \bar{U}_L \bar{\rho}(t) \bar{U}_2^T & \cdots & \bar{U}_L \bar{\rho}(t) \bar{U}_L^T \end{bmatrix}, \end{aligned}$$

so we have

$$\begin{aligned} \bar{\rho}(t+1) &= (\bar{U} \bar{\rho}(t) \bar{U}^T) \\ &= [\bar{U}_1 \bar{\rho}(t) \bar{U}_1^T \quad \bar{U}_2 \bar{\rho}(t) \bar{U}_1^T \quad \cdots \quad \bar{U}_L \bar{\rho}(t) \bar{U}_1^T \\ &\quad \cdots \quad \bar{U}_1 \bar{\rho}(t) \bar{U}_L^T \quad \cdots \quad \bar{U}_L \bar{\rho}(t) \bar{U}_L^T]^T. \end{aligned}$$

Obviously,

$$\tilde{\rho}(t) = \begin{bmatrix} \bar{\rho}_1 \\ \bar{\rho}_2 \\ \vdots \\ \bar{\rho}_L \end{bmatrix},$$

then

$$\tilde{U} \tilde{\rho}(t) = \bar{U} \otimes \bar{U} \tilde{\rho}(t) = \begin{bmatrix} \bar{U}_1 \otimes \bar{U}_1 \bar{\rho}(t) \\ \bar{U}_1 \otimes \bar{U}_2 \bar{\rho}(t) \\ \vdots \\ \bar{U}_1 \otimes \bar{U}_L \bar{\rho}(t) \\ \vdots \\ \bar{U}_L \otimes \bar{U}_1 \bar{\rho}(t) \\ \vdots \\ \bar{U}_L \otimes \bar{U}_L \bar{\rho}(t) \end{bmatrix},$$

where

$$\begin{aligned}\bar{U}_i \otimes \bar{U}_j \tilde{\rho}(t) &= [\bar{U}_{i,1} \quad \bar{U}_{i,2} \quad \cdots \quad \bar{U}_{i,L}] \otimes \bar{U}_j \begin{bmatrix} \tilde{\rho}_1 \\ \tilde{\rho}_2 \\ \vdots \\ \tilde{\rho}_L \end{bmatrix} = [\bar{U}_{i,1}\bar{U}_j \quad \bar{U}_{i,2}\bar{U}_j \quad \cdots \quad \bar{U}_{i,L}\bar{U}_j] \begin{bmatrix} \tilde{\rho}_1 \\ \tilde{\rho}_2 \\ \vdots \\ \tilde{\rho}_L \end{bmatrix} \\ &= \bar{U}_{i,1}\bar{U}_j\tilde{\rho}_1 + \bar{U}_{i,2}\bar{U}_j\tilde{\rho}_2 + \cdots + \bar{U}_{i,L}\bar{U}_j\tilde{\rho}_L = \bar{U}_{i,1}\tilde{\rho}_1^T\bar{U}_j^T + \bar{U}_{i,2}\tilde{\rho}_2^T\bar{U}_j^T + \cdots + \bar{U}_{i,L}\tilde{\rho}_L^T\bar{U}_j^T \\ &= \bar{U}_i \begin{bmatrix} \tilde{\rho}_1^T \\ \tilde{\rho}_2^T \\ \vdots \\ \tilde{\rho}_L^T \end{bmatrix} \bar{U}_j^T.\end{aligned}$$

Since $\tilde{\rho}(t)$ is a symmetric matrix, we have

$$\tilde{\rho}(t) = \begin{bmatrix} \tilde{\rho}_1^T \\ \tilde{\rho}_2^T \\ \vdots \\ \tilde{\rho}_L^T \end{bmatrix}.$$

Therefore, the original expression becomes $\bar{U}_i \otimes \bar{U}_j \tilde{\rho}(t) = \bar{U}_i \tilde{\rho}(t) \bar{U}_j^T$. Thus, we have

$$\tilde{U} \tilde{\rho}(t) = \begin{bmatrix} \bar{U}_1 \tilde{\rho}(t) \bar{U}_1^T \\ \bar{U}_1 \tilde{\rho}(t) \bar{U}^T \\ \vdots \\ \bar{U}_1 \tilde{\rho}(t) \bar{U}_L^T \\ \vdots \\ \bar{U}_L \tilde{\rho}(t) \bar{U}_1^T \\ \vdots \\ \bar{U}_L \tilde{\rho}(t) \bar{U}_L^T \end{bmatrix},$$

and by $\bar{U}_i \tilde{\rho}(t) \bar{U}_j^T = \bar{U}_j \tilde{\rho}(t) \bar{U}_i^T$ we know that $\tilde{U} \tilde{\rho}(t) = \tilde{\rho}(t+1)$. The proof is complete. Obviously, $\tilde{\rho}(t) = (\tilde{U})^t \tilde{\rho}(0)$.

B. Szegedy's quantum network source-location model

We assume that we can only observe the probability \mathbf{P}_O that the quantum walker is located at n observe nodes $O = \{o_1, o_2, \dots, o_n\}$ at some discrete time steps, which start from t for k consecutive time steps, so the source-location model is

$$\begin{aligned}\mathbf{P}_O &= \begin{pmatrix} \mathbf{P}_O(t_0 + t) \\ \mathbf{P}_O(t_0 + t + 1) \\ \vdots \\ \mathbf{P}_O(t_0 + t + k - 1) \end{pmatrix} \\ &= \begin{pmatrix} D\bar{B}W\tilde{U}^{t_0+t} \\ D\bar{B}W\tilde{U}^{t_0+t+1} \\ \vdots \\ D\bar{B}W\tilde{U}^{t_0+t+k-1} \end{pmatrix} \tilde{\rho}(t_0),\end{aligned}\quad (11)$$

where t_0 is the initial time of the quantum network system, t is the start time of observation, and k is the number of time steps of continuous observation. Matrix W is used to extract

the probability part of $\tilde{\rho}$, that is, the main diagonal elements in the original $\tilde{\rho}$. The dimension of W is $L \times L^2$, and in the i th row of W , only the $(i \times L + i - m)$ th element is one. D is the observer matrix with dimension $n \times N$; each row of D corresponds to an observer node, the k^{o_i} th element of the i th row is one, and the other elements are zero, k^{o_i} is the serial number of observer node o_i . For a network, the maximum dimension of the observer matrix D can be $N \times N$, that is, we observe the probability that the quantum walker is located at all nodes in the network. We can solve vector $\tilde{\rho}(t_0)$ using the observed vector \mathbf{P}_O and known matrix

$$\begin{pmatrix} D\bar{B}W\tilde{U}^{t_0+t} \\ D\bar{B}W\tilde{U}^{t_0+t+1} \\ \vdots \\ D\bar{B}W\tilde{U}^{t_0+t+k-1} \end{pmatrix}$$

according to Eq. (11). Figure 3 shows a schematic diagram of Szegedy's quantum network source-location model. Figure 3(a) shows a simple network consisting of seven nodes and eight edges. The number inside the node is the serial number of the node, and the number next to the edge is the serial number of the directed edge. Now the Szegedy's quantum walk is carried out on this network, the source node is v_4 (red), the observer node is v_1 (blue), v_3 (green), and v_6 (purple), the serial number of the directed edge starting from v_1 , v_3 , and v_6 is also marked the same color as nodes, which means that the quantum walker locating at a node is equivalent to locating at the directed edges which start from this node. It can be seen that the directed edges corresponding to the source node v_4 are $a_{4,3}$, $a_{4,6}$, and $a_{4,7}$, and these three edges all start from node v_4 , their serial numbers are 7, 8, and 9, respectively. The subimage on the left side of the network is a schematic diagram of the evolutionary process from $\tilde{\rho}(0)$ to $\tilde{\rho}(t)$ by \tilde{U}^t during Szegedy's quantum walk on the network. At the initial time, the quantum walker is located at the superposition state of these three directed edges, and the probability of locating at each edge is $1/3$, the positions of three probability values $1/3$ in $\tilde{\rho}(0)$ are 103, 120, and 137, respectively. Obviously, the observer node set is $O = \{v_1, v_3, v_6\}$. Similarly, the directed edges corresponding to observer nodes v_1 are $a_{1,2}$, $a_{1,3}$, and $a_{1,6}$, the directed edges corresponding to observer nodes v_3 are $a_{3,1}$ and $a_{3,4}$, and the directed edges corresponding to observer nodes v_6 are $a_{6,1}$, $a_{6,4}$, $a_{6,5}$, and $a_{6,7}$. The vector $W\tilde{\rho}(t)$ on the right side of the network is the probability of the

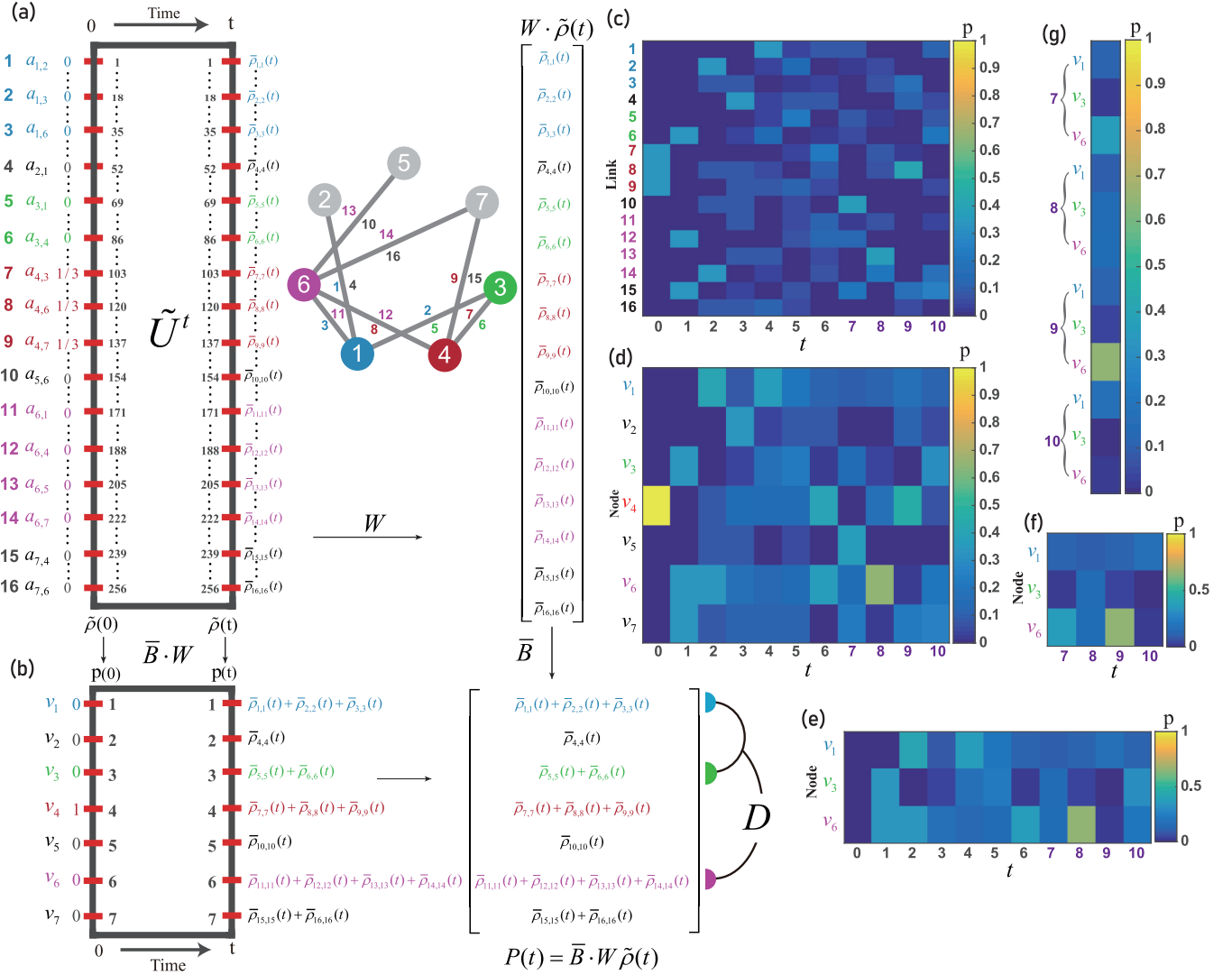


FIG. 3. Schematic diagram of Szegedy's quantum network source-location model. (a) A simple network consisting of seven nodes and eight edges. (b) The result of converting the probability of the quantum walker locate at edges to nodes after operation of $\bar{B}W$. (c) The probability evolution process of the quantum walker being located at different directed edges during Szegedy's quantum walk on the network in panel (a). (d) The result of converting the probability of the quantum walker being located at directed edges in panel (c) to nodes. (e) The probabilities at different time steps of the quantum walker being located at observer nodes. (f) The probability evolution on observer nodes at the time steps. (g) The result of converting the observer nodes probability in panel (f) into a column vector.

quantum walker being located at each directed edge, namely, the main diagonal element in the original $\tilde{\rho}(t)$. The dimension of W is 16×256 . Figure 3(b) is the result of converting the probability of the quantum walker located at edges to nodes after operation of $\bar{B}W$. Moreover, v_1 , v_3 , and v_6 are observer nodes at time t , that is, the probability of the quantum walker being located at node v_1 is $\tilde{\rho}_{1,1}(t) + \tilde{\rho}_{2,2}(t) + \tilde{\rho}_{3,3}(t)$, the probability of the quantum walker being located at node v_3 is $\tilde{\rho}_{5,5}(t) + \tilde{\rho}_{6,6}(t)$, and the probability of the quantum walker being located at node v_6 is $\tilde{\rho}_{11,11}(t) + \tilde{\rho}_{12,12}(t) + \tilde{\rho}_{13,13}(t) + \tilde{\rho}_{14,14}(t)$. In this case, the observer matrix is

$$D = \begin{bmatrix} 1 & 0 & 0 & 0 & 0 & 0 & 0 \\ 0 & 0 & 1 & 0 & 0 & 0 & 0 \\ 0 & 0 & 0 & 0 & 0 & 1 & 0 \end{bmatrix}.$$

Figure 3(c) shows the probability evolution process of the quantum walker being located at different directed edges during Szegedy's quantum walk on the network in Fig. 3(a). The abscissa is a discrete time step, the ordinate is the serial number of the directed edge, and the colors in the heat map correspond to the probability of the quantum walker being located at the directed edge. At each time step, the quantum walker is located at the superposition state of multiple directed edges. Figure 3(d) shows the result of converting the probability of the quantum walker being located at the directed edges in Fig. 3(c) to nodes. Figure 3(e) shows the probabilities at different time steps of the quantum walker being located at observer nodes v_1 , v_3 , and v_6 that are extracted from the matrix in Fig. 3(d); that is, rows 1, 3, and 6 in Fig. 3(d) are extracted. Figure 3(f) shows the probability evolution on observer nodes at time steps $t = 7, 8, 9, 10$ that are extracted

from Fig. 3(e); that is, the columns $t = 7, 8, 9, 10$ in Fig. 3(e) are extracted. Figure 3(g) is the result of converting the observer nodes probability in Fig. 3(f) into a column vector; that is, all columns are used to form a column vector

$$\begin{pmatrix} \mathbf{P}_O(7) \\ \mathbf{P}_O(8) \\ \mathbf{P}_O(9) \\ \mathbf{P}_O(10) \end{pmatrix},$$

which is treated as

$$\begin{pmatrix} \mathbf{P}_O(t_0 + t) \\ \mathbf{P}_O(t_0 + t + 1) \\ \vdots \\ \mathbf{P}_O(t_0 + t + k - 1) \end{pmatrix}$$

in the source-location model (11), and this is the observer information for locating quantum network sources.

IV. APPROXIMATE SIMPLIFIED SOURCE-LOCATION MODEL

In the linear Szegedy's quantum network system evolution equation, that is, Eq. (10), the unitary evolution matrix change from \tilde{U} with dimensions $L \times L$ to \hat{U} with dimensions $L^2 \times L^2$, and this results in a high complexity of the source-location task. In view of these difficulties, we consider reasonably simplifying the source-location model (11) in this section. First, we swap the rows and columns of the matrix \tilde{U} at the same time and finally obtain a block matrix of the following form:

$$\hat{U} = \begin{bmatrix} \tilde{U}^\dagger \cdot \tilde{U} & \Delta_1 \\ \Delta_2 & \Delta_3 \end{bmatrix}, \quad (12)$$

where $\tilde{U}^\dagger \cdot \tilde{U}$ means that the elements at the corresponding positions of the two matrices are multiplied, and the $\tilde{\rho}$ corresponding to \hat{U} takes the form

$$\tilde{\rho} = \begin{bmatrix} \tilde{\rho}_{1,1}(t) \\ \tilde{\rho}_{2,2}(t) \\ \vdots \\ \tilde{\rho}_{L,L}(t) \\ \vdots \end{bmatrix}. \quad (13)$$

We get the evolution equation

$$\begin{aligned} \hat{U} \tilde{\rho} &= \begin{bmatrix} \tilde{U}^\dagger \cdot \tilde{U} & \Delta_1 \\ \Delta_2 & \Delta_3 \end{bmatrix} \begin{bmatrix} \tilde{\rho}_{1,1}(t) \\ \tilde{\rho}_{2,2}(t) \\ \vdots \\ \tilde{\rho}_{L,L}(t) \\ \vdots \end{bmatrix} \\ &= \begin{bmatrix} \tilde{\rho}_{1,1}(t+1) \\ \tilde{\rho}_{2,2}(t+1) \\ \vdots \\ \tilde{\rho}_{L,L}(t+1) \\ \vdots \end{bmatrix}. \end{aligned} \quad (14)$$

Then we omit Δ_2 and Δ_3 , and let $\Delta_1 = I$ (I is an identity matrix with dimension $L \times L$), then we get the simplified approximate evolution as

$$\begin{aligned} \hat{U} \tilde{\rho} &= [\tilde{U}^\dagger \cdot \tilde{U} \quad I] \begin{bmatrix} \tilde{\rho}_{1,1}(t) \\ \tilde{\rho}_{2,2}(t) \\ \vdots \\ \tilde{\rho}_{L,L}(t) \\ \mathbf{\Omega}(t) \end{bmatrix} \\ &= \begin{bmatrix} \tilde{\rho}_{1,1}(t+1) \\ \tilde{\rho}_{2,2}(t+1) \\ \vdots \\ \tilde{\rho}_{L,L}(t+1) \end{bmatrix} = \mathbf{P}(t+1), \end{aligned} \quad (15)$$

where the dimension of $[\tilde{U}^\dagger \cdot \tilde{U} \quad I]$ is $L \times 2L$,

$$\begin{bmatrix} \tilde{\rho}_{1,1}(t) \\ \tilde{\rho}_{2,2}(t) \\ \vdots \\ \tilde{\rho}_{L,L}(t) \\ \mathbf{\Omega}(t) \end{bmatrix}$$

is a vector with dimensions $2L \times 1$, and $\mathbf{\Omega}(t)$ is an unknown vector with L elements. Model (15) is the logical approximation of model (10) without changing its evolution principle, and which also dramatically reduces computational and space complexity. Figure 4 is the diagram of the obtain simplified Model (15). Figure 4(a) shows a simple network with three nodes including v_1 , v_2 , and v_3 . The numbers in nodes are the serial number of nodes and nodes v_1 and v_2 are sources (red); that is, the quantum walker is located at the superposition state of nodes v_1 and v_2 at the initial time. Figure 4(b) shows the state of Szegedy's quantum walk on the network in Fig. 4(a) at the initial time. $|\tilde{\psi}(0)\rangle$ is the reduced initial state vector, namely, the initial wave function. In the simulation below, we set the probability of the quantum walker located at each source node the same at the initial time, and the probability of the walker locate at all edges corresponding to a node is equal. $\tilde{\mathbf{P}}(0)$ is the corresponding probability, we use the symbols O, Δ , Θ , and Ξ to represent the four values in $\tilde{\mathbf{P}}(0)$. $\tilde{\rho}(0)$ is the density matrix corresponding to $|\tilde{\psi}(0)\rangle$, and $\tilde{\rho}(0)$ is the vectorization of $\tilde{\rho}(0)$. Figure 4(c) shows the system state evolution equation of Szegedy's quantum walk on the network in Fig. 4(a). The four rows of elements numbered 1 (red squares), 2 (purple squares), 3 (blue squares), and 4 (green squares) in \tilde{U}^t are respectively operated with $\tilde{\rho}(0)$ to get the elements in $\tilde{\rho}(t)$ which are marked as squares colored red, purple, blue, and green. In the product operation of matrix \tilde{U}^t and vector $\tilde{\rho}(0)$, the four column elements numbered 1, 2, 3, 4 in \tilde{U}^t will be multiplied by the four symbols O, Δ , Θ , and Ξ in $\tilde{\rho}(0)$, respectively. Figure 4(d) is obtained by elementary transformation L^{-1} of \tilde{U}^t in Fig. 4(c), that is, the rows in \tilde{U}^t are exchanged, and the rows marked 1 (red), 2 (purple), 3 (blue), and 4 (green) are arranged at the front, then the corresponding probability in $\tilde{\rho}(t)$ is also at the top. Figure 4(e) is to perform an elementary transformation L on the evolution matrix in Fig. 4(d), that is, exchange the columns

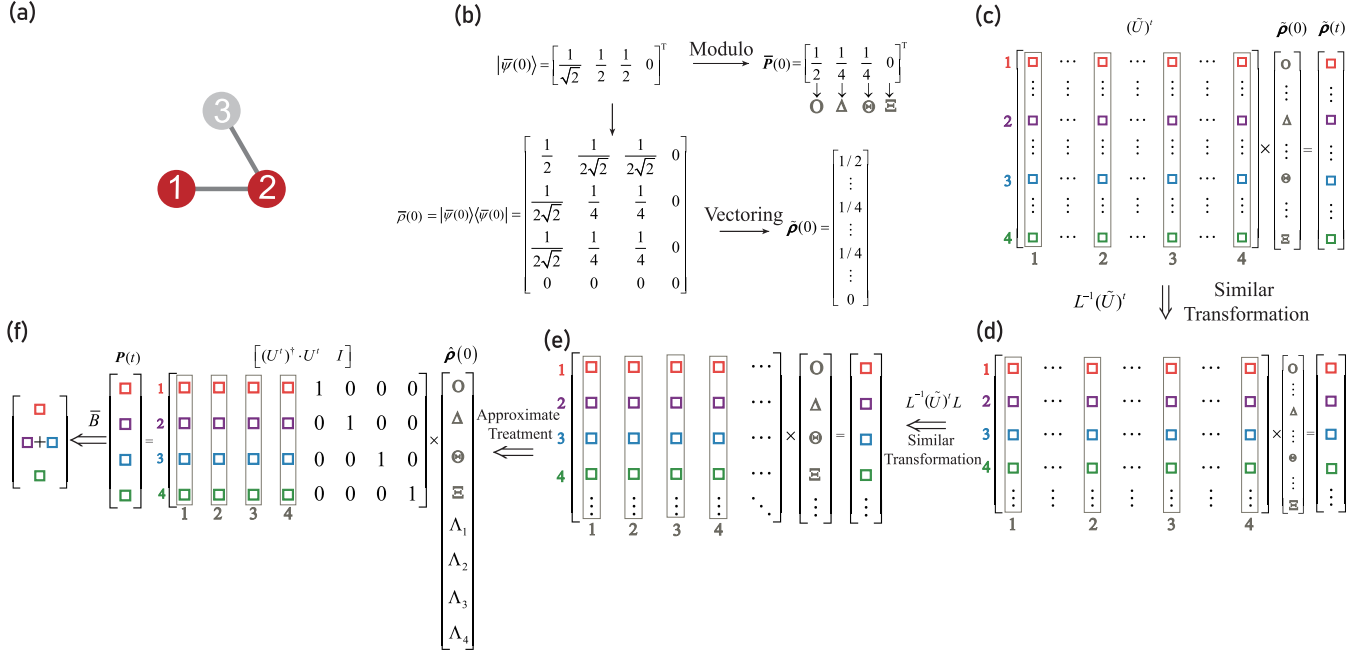


FIG. 4. The diagram of a simplified quantum network source-location model. (a) A simple network with three nodes. (b) The state of Szegedy's quantum walk on the network in panel (a) at the initial time. (c) The system state evolution equation of Szegedy's quantum walk on the network in panel (a). (d) Obtained by elementary transformation L^{-1} of \tilde{U}^t in panel (c). (e) Perform elementary transformation L on the evolution matrix in panel (d). (f) An approximate simplification of panel (e).

of $L^{-1}(\tilde{U})^t$, so that the columns 1, 2, 3, 4 are ranked at the front, and the corresponding probability in $\tilde{\rho}(0)$ is also ranked at the top. After Figs. 4(c) to 4(e), the similar transformation of matrix \tilde{U}^t is completed, and the probabilities in $\tilde{\rho}(0)$ and $\tilde{\rho}(t)$ are ranked at the top. Figure 4(f) shows an approximate simplification of Fig. 4(e). Only the part of the probability value is retained in $\tilde{\rho}(t)$, and then replaced with $\mathbf{P}(t)$, so only the first four rows of elements are retained in the evolution matrix $L^{-1}(\tilde{U})^t L$ after similarity transformation, and the elements of nonprobability part in $\tilde{\rho}(0)$ are simplified to four elements, marked with four symbols $\Lambda_1, \Lambda_2, \Lambda_3$, and Λ_4 , we denote the part of the evolution matrix corresponding to these four symbols as an identity matrix I . So the final approximate simplified evolution equation is

$$[(\tilde{U}^t)^\dagger \tilde{U}^t \quad I] \begin{bmatrix} \tilde{\rho}_{1,1}(0) \\ \tilde{\rho}_{2,2}(0) \\ \vdots \\ \tilde{\rho}_{L,L}(0) \\ \mathbf{\Omega}(0) \end{bmatrix} = \begin{bmatrix} \tilde{\rho}_{1,1}(t) \\ \tilde{\rho}_{2,2}(t) \\ \vdots \\ \tilde{\rho}_{L,L}(t) \end{bmatrix} = \mathbf{P}(t)$$

or

$$[\tilde{U}^\dagger \tilde{U} \quad I] \begin{bmatrix} \tilde{\rho}_{1,1}(t) \\ \tilde{\rho}_{2,2}(t) \\ \vdots \\ \tilde{\rho}_{L,L}(t) \\ \mathbf{\Omega}(t) \end{bmatrix} = \begin{bmatrix} \tilde{\rho}_{1,1}(t+1) \\ \tilde{\rho}_{2,2}(t+1) \\ \vdots \\ \tilde{\rho}_{L,L}(t+1) \end{bmatrix} = \mathbf{P}(t+1),$$

where

$$\mathbf{\Omega} = \begin{bmatrix} \Lambda_1 \\ \Lambda_2 \\ \Lambda_3 \\ \Lambda_4 \end{bmatrix}$$

in this diagram. Finally, the probability of the quantum walker locate at nodes is obtained after the operation of matrix \tilde{B} on $\mathbf{P}(t)$.

The simplified source-location model is then

$$\begin{pmatrix} \mathbf{P}_O(t_0+t) \\ \mathbf{P}_O(t_0+t+1) \\ \vdots \\ \mathbf{P}_O(t_0+t+k-1) \end{pmatrix} = \begin{pmatrix} D\tilde{B}\hat{U}^{t_0+t} \\ D\tilde{B}\hat{U}^{t_0+t+1} \\ \vdots \\ D\tilde{B}\hat{U}^{t_0+t+k-1} \end{pmatrix} \hat{\rho}(t_0)t. \quad (16)$$

We assume that the source is sparse; that is, Szegedy's quantum walker starts from a superposition of s source nodes, and n is much smaller than N at the initial time. So $\tilde{\rho}(t_0)$ in Eq. (11) and $\hat{\rho}(t_0)$ in Eq. (16) are sparse vectors. Then we can use compressed sensing theory [31,32] to solve the original source-location Model (11) and its simplified Model (16). Please refer to Algorithm 1 for the detailed process of solving models (11) and (16) [33,34].

Algorithm 1: Szegedy's quantum network source location based on compressed sensing.

Input : $\begin{pmatrix} D\bar{B}W\tilde{U}^{t_0+t} \\ D\bar{B}W\tilde{U}^{t_0+t+1} \\ \vdots \\ D\bar{B}W\tilde{U}^{t_0+t+k-1} \end{pmatrix}$ and $\begin{pmatrix} \mathbf{P}_O(t_0+t) \\ \mathbf{P}_O(t_0+t+1) \\ \vdots \\ \mathbf{P}_O(t_0+t+k-1) \end{pmatrix}$ in Equation (11) of original model or $\begin{pmatrix} D\bar{B}\hat{U}^{t_0+t} \\ D\bar{B}\hat{U}^{t_0+t+1} \\ \vdots \\ D\bar{B}\hat{U}^{t_0+t+k-1} \end{pmatrix}$ and $\begin{pmatrix} \mathbf{P}_O(t_0+t) \\ \mathbf{P}_O(t_0+t+1) \\ \vdots \\ \mathbf{P}_O(t_0+t+k-1) \end{pmatrix}$ in Equation (16) of simplified model.

Output : $\tilde{\rho}(t_0)$ in Equation (11) of original model or $\hat{\rho}(t_0)$ in Equation (16) of simplified model.

Initialization: First, express the problem of Equation (11) or (16) as the minimization of the L1 norm $\|\tilde{\rho}(t_0)\|_1$ or $\|\hat{\rho}(t_0)\|_1$, and provide the constraint conditions of Equation (11) or Equation (16). Then, rephrase it in the form of a dual problem as linear programming, minimizing $sum(\mathbf{u})$, and adding the constraint conditions $-\mathbf{u} \leq \tilde{\rho}(t_0) \leq \mathbf{u}$ and Equation (11) or $-\mathbf{u} \leq \hat{\rho}(t_0) \leq \mathbf{u}$ and Equation (16), where \mathbf{u} is an intermediate variable with the same dimension as $\tilde{\rho}(t_0)$ or $\hat{\rho}(t_0)$ [33,34]. Initialize the following parameters: the initial point of the algorithm is $\tilde{\rho}$ or $\hat{\rho}$, the termination tolerance of the primal-dual algorithm is $tolerance = 10^{-3}$, the maximum number of iterations of the primal-dual algorithm is $max_iterations = 50$, the step size factor of the backtracking line search algorithm is $step_size$, the growth rate of the backtracking line search step size factor is $growth_rate$, the convergence measure of duality gap is $duality_gap(\tilde{\rho})$ or $duality_gap(\hat{\rho})$, and the initial number of iterations is $iterations = 0$.

- 1 **while** $duality_gap \geq tolerance$ or $iterations \leq max_iterations$ **do**
- 2 Determine the search direction $search_direction$ using the conjugate gradient method search.
- 3 Obtain the step length $step_length(step_size, growth_rate)$ using the backtracking line search method.
- 4 Update intermediate variables.
- 5 Update variables $\tilde{\rho}(search_direction, step_length)$ or $\hat{\rho}(search_direction, step_length)$.
- 6 Update $duality_gap(\tilde{\rho})$ or $duality_gap(\hat{\rho})$.
- 7 Update $iterations = iterations + 1$.
- 8 **end**

For the simplified model in Eq. (16), the time complexity of this algorithm consists of two main components: one is the complexity of each iteration, and the other is the number of iterations required. Assume the size of $\hat{\rho}(t_0)$ is $2L$. In each iteration, the most time-consuming operation is typically determining the search direction and step size. The complexity of determining the step size using the backtracking line search method depends on the number of algorithm searches and has a worst-case complexity of $O(L^3)$. The time complexity of computing intermediate variables, updating variables, and other operations is at most $O(L)$. Finally, considering the number of algorithm cycles as K , the worst-case time complexity is $O(KL^3)$. For the original model in Eq. (11), the algorithm's time complexity can be as high as $O(KL^6)$. We implement algorithms by using MATLAB programming language and all of the simulations below are run on a ThinkCentre M720t machine with 8 GB primary memory and a core i5 (CPU 3 GHz) processor.

V. RESULTS

To quantify the validity and efficiency of the proposed quantum network source-location algorithm based on limited information of observer nodes, we study the success rate of locating sources on both model and real networks. Model networks are BA scale-free networks (BA) [35], ER random networks (ER) [36], and WS small world networks (WS) [37] with size $N = 50$ and average degree $\langle K \rangle = 4$. Real static networks include Gold [38], Karate [39], Dolphins [40], and Prison [41]. During simulations in this paper, observer nodes and sources are selected randomly except where noted. The number of sources s represents that the quantum walker is in the superposition state of s source nodes at the initial time. Here a standard metric, the area under the receiver operating characteristic curve (AUC) [42], is used to quantify the accuracy of our algorithm. We first rank the nodes based on their reconstructed probability values in $\mathbf{P}(0)$ in ascending order and obtain a new candidate list. The AUC is calculated by

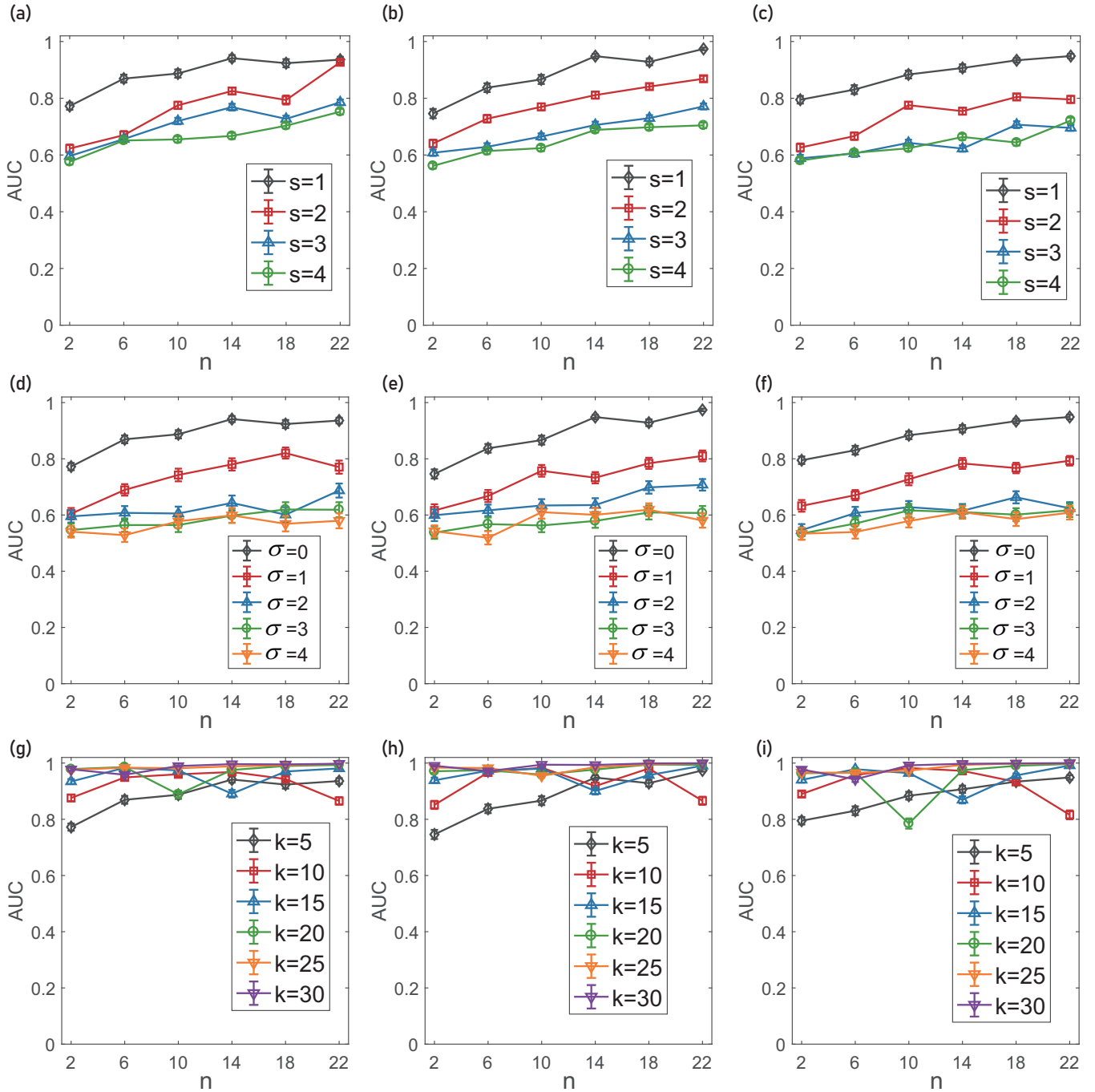


FIG. 5. Accuracy of locating sources on model networks. (a)–(c) The influence of number of sources on locating result on model networks. The number of observer time steps is fixed as five, and the noise standard deviation is zero. The abscissa is the number of observer nodes, ordinate is the AUC value, and curves of different colors corresponding to the source-location results of different number of sources. Error bars represent the standard error. (d)–(f) The influence of different noise on source-location accuracy. We fix observer time steps as five, and the number of sources is one. Curves of different colors corresponding to different noise standard deviations σ . (g)–(i) The influence of different observer time steps on source-location accuracy. Different curves corresponding to different observer time steps. The number of sources is fixed as one, and the standard deviation of noise is zero. (a), (d), (g) Results of the BA network. (b), (e), (h) Results of ER network. (c), (f), (i) Results of WS network.

two indexes, true positive rate (TPR) and false positive rate (FPR). TPR is $TPR(l) = \frac{TP(l)}{s}$, where $TP(l)$ is the number of true sources in the top l nodes of candidate list, s is the number of sources. FPR is $FPR(l) = \frac{FP(l)}{N-s}$, where $FP(l)$ is the number of false positives in the top l nodes of candidate list. The

abscissa of receiver operating characteristic curve is FPR and ordinate is TPR, AUC is the area under this curve. The higher the AUC, the better the location performance of the algorithm. All results for the AUC are mean values of 100 repeated simulations. In practice, most real quantum systems are not closed

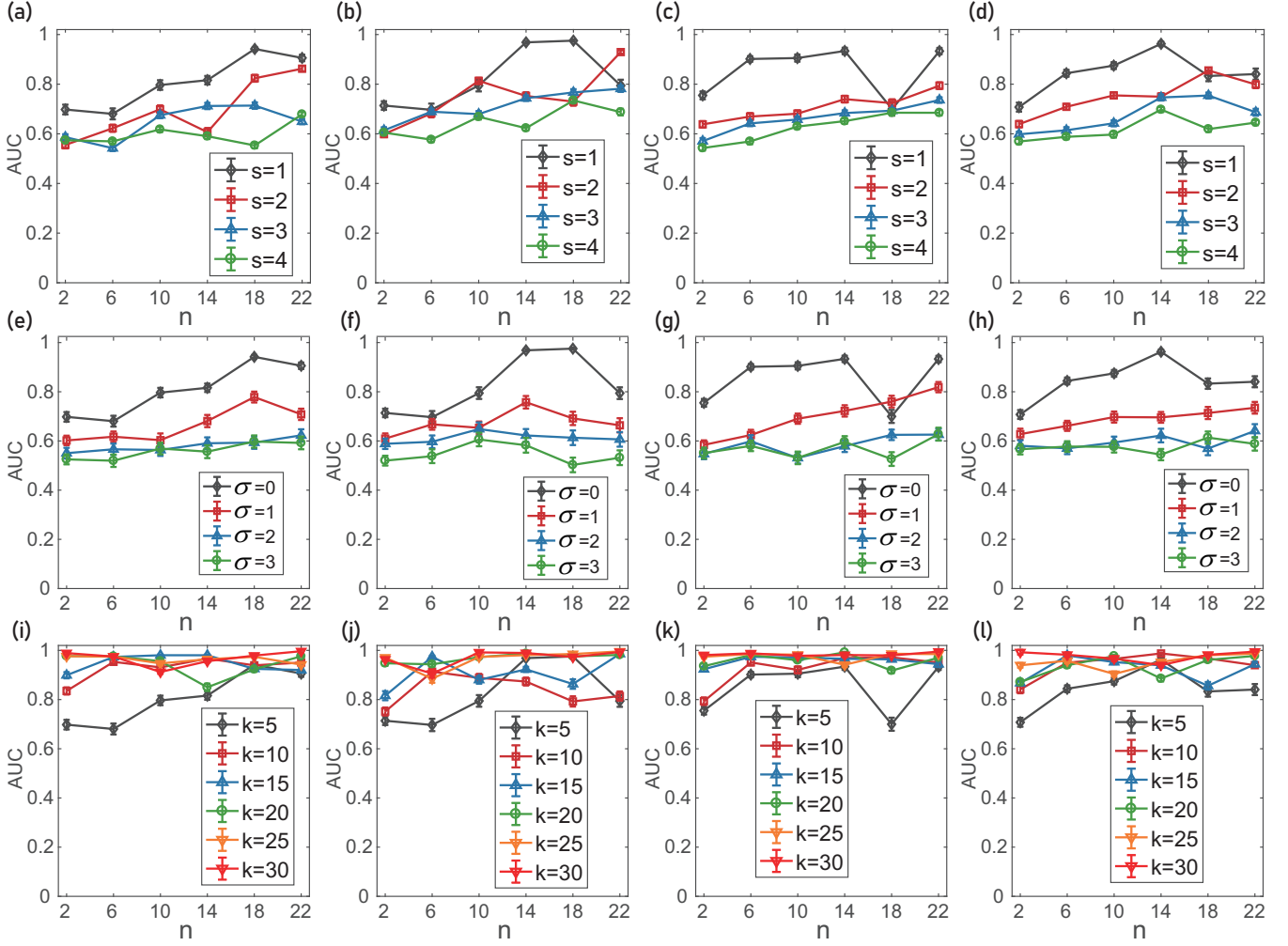


FIG. 6. Accuracy of locating sources on real networks. (a)–(d) Influence of number of sources on locating result on model networks. The number of observer time steps is fixed as five, and the noise standard deviation is zero. (e)–(h) Influence of different noise on source-location accuracy. We fix observer time steps as five, and the number of source is one. (i)–(l) Influence of different observer time steps on source-location accuracy. The number of sources is fixed as one, and the standard deviation of noise is zero. (a), (e), (i) Results of Gold network. (b), (f), (j) Results of Karate network. (c), (g), (k) Results of Dolphins network. (d), (h), (l) Results of Prison network.

quantum systems and are more sensitive to external environments, the observer information is generally unpurified, so in order to verify the robustness of the algorithm, we consider adding Gaussian white noise to the observation information [25], i.e., the observer information is $\hat{\mathbf{P}} = [I + N(0, \sigma^2 I)]\mathbf{P}$, and adjust the size of the noise by changing the standard deviation σ of Gaussian noise. When σ increases, the noise increases. The difficulty of source-location accuracy increases.

Figures 5–7 show the simulation results of the proposed source-location algorithm on model and empirical networks. Figure 5 shows the accuracies of source location on model networks. As we can see, the performance of our method increases with the number of observer nodes increasing. As can be seen from Figs. 5(a)–5(c), the difficulty of locating sources increases with the increase of the number of sources on different model networks. For the case of one source, with only approximately 6 observer nodes, which accounts for 12% of the total observer nodes, we can receive relatively high accuracy $AUC > 0.8$. From Figs. 5(d)–5(f), it

can be seen that, with the increase of noise, the difficulty of locating sources gradually increases. When the standard deviation of noise $\sigma > 1$, the accuracy of locating sources decreases sharply and the algorithm is close to failure. While for $\sigma \leq 1$, good locating results can still be obtained, which indicates that the algorithm has tolerable robustness. Figures 5(g)–5(h) show the influence of different observer time steps on the source-location accuracy. It can be seen that the source-location accuracy increases with the increase of the number of observer time steps. However, when the number of observer nodes is sufficient, the influence of observer time steps on source-location accuracy is weakened. Figure 6 shows the accuracies of source location on real networks. In general, the proposed quantum network source-location algorithm can perform well on different model and real networks. Figure 7 compares source-location accuracy on different networks. It can be seen from Figs. 7(a)–7(h) that the source-location accuracy of the proposed algorithm has not much difference for different model networks and ac-

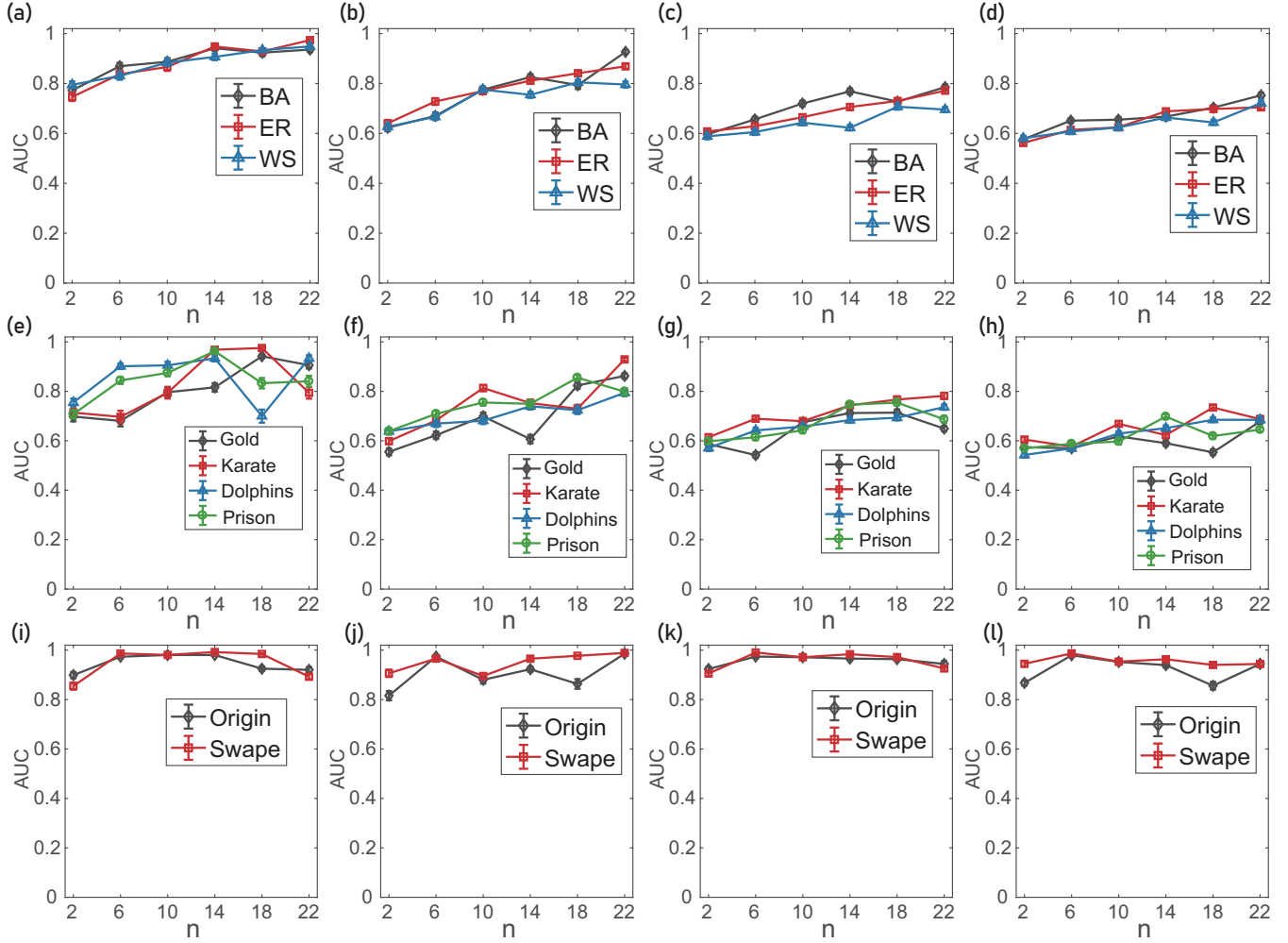


FIG. 7. Comparison of source-location accuracy on different networks. (a)–(d) Simulation results on different model networks. Curves of different colors corresponding to different model networks. Error bars represent the standard error. The number of observer time steps is fixed as five, and the noise standard deviation is zero, the number of sources in panel (a) is 1, in (b) is 2, in (c) is 3, and in (d) is 4. (e)–(h) Simulation results on different real networks. Curves of different colors corresponding to different real networks. The other parameters are set in the same way as for the model network. (i)–(l) Influence of network properties except degree distribution on source-location accuracy. The black curve is the source-location accuracy on the original network, and the red curve is source-location accuracy on the swapped network. The number of observer time steps is fixed as 15, the noise standard deviation is zero, and the number of sources is one. (i) Result of Gold network. (j) Result of Karate network, (k) Result of Dolphins network. (l) Result of Prison network.

tual networks. In addition, we also study how other network properties except degree distribution affect source-location accuracy. We randomly swap all edges and preserve the degree sequence of real networks. Moreover, it can be seen from Figs. 7(i)–7(l) that other properties except degree distribution do not affect the source-location accuracy of the proposed algorithm.

Figure 8 is the comparison of source-location accuracy between original model and simplified model. It can be observed that the source-location accuracy of the simplified model is slightly lower compared with that of the original model. However, when the number of observed nodes is sufficiently large, the source-location accuracy of both models is essentially comparable. Compared with the original model, the simplified model exhibits a decrease in the overall average source-location accuracy by 5.16% on BA networks. The average source-location accuracy decreases by 1.68%

for observed node numbers ranging from 12 to 18. On ER networks, the simplified model shows a decrease in the overall average source-location accuracy by 6.28%. The average source-location accuracy decreases by 1.72% for observed node numbers ranging from 12 to 18. On WS networks, the simplified model experiences a decrease in the overall average source-location accuracy by 7.43%. The average source-location accuracy decreases by 3.06% for observed node numbers ranging from 12 to 18. Overall, the source-location accuracy of the simplified model is considered to meet expectations.

VI. DISCUSSION

In this paper, we present a highly precise and robust source-location algorithm for quantum networks based on compressive sensing. Our proposed algorithm effectively

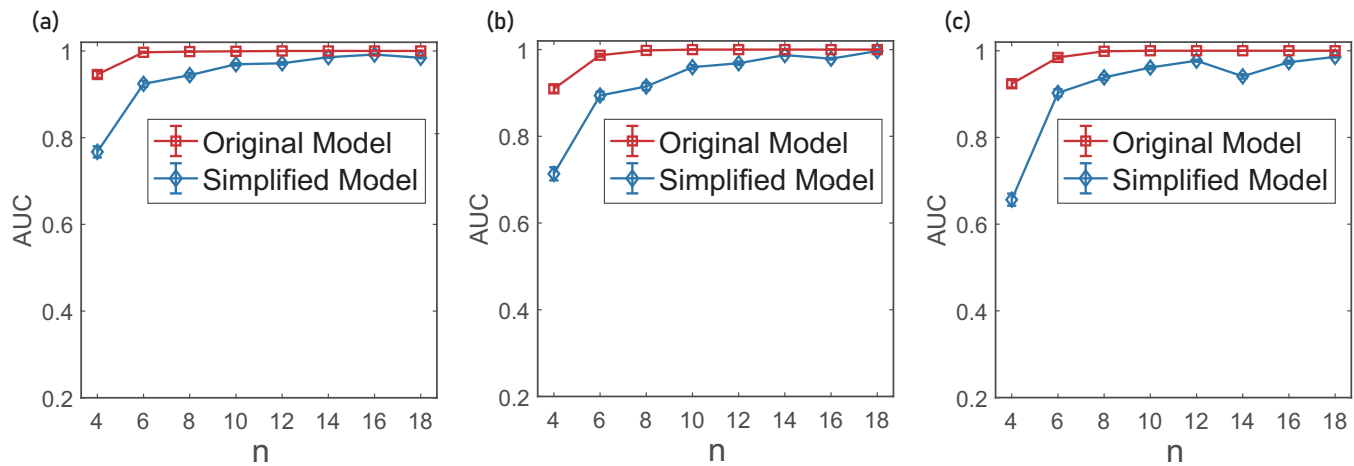


FIG. 8. Comparison of source-location accuracy between the original model and the simplified model. Curves of different colors corresponding to different source-location models. Error bars represent the standard error. The number of observer time steps is fixed as 20, the noise standard deviation is zero, the number of sources is two. (a)–(c) Simulation results on BA, ER, and WS networks, respectively.

determines the locations of sources in both model and real networks with diverse topologies, utilizing limited observer nodes. Through simulations, we demonstrate the satisfactory performance of our algorithm under varying conditions, including different numbers of observer nodes, observer time steps, noise levels, network structures, and numbers of sources. Nevertheless, there are several areas where further improvements can be made. First, the proposed algorithm assumes knowledge of the initial time of sources, whereas in practical scenarios, this information is often unknown. Second, while the observer nodes in our study are randomly selected, determining the optimal number and placement of observer nodes to enhance the algorithm's accuracy and efficiency warrants further investigation. Lastly, despite reducing the original Szegedy's quantum walk and simplifying the algorithm reasonably, additional efforts are necessary to enhance the efficiency of the proposed algorithm for large-scale complex networks.

The datasets used and analyzed during the current study are available from the corresponding author upon reasonable request.

ACKNOWLEDGMENTS

This work is supported by the Youth Fund of Beijing Wuzi University (Grant No. 2021XJQN05). The authors would like to express their sincere appreciation to Wang Wenxu, Xu Hongya, Ying-Cheng Lai, and Zhang Xiaoxiao for their detailed and helpful comments to improve the quality of the paper.

All authors contributed equally to this work.

The authors declare that they have no known competing financial interests or personal relationships that could have appeared to influence the work reported in this paper.

- [1] J. Biamonte, M. Faccin, and M. De Domenico, Complex networks from classical to quantum, *Commun. Phys.* **2**, 53 (2019).
- [2] D. Oren, M. Mutzafi, Y. C. Eldar, and M. Segev, Quantum state tomography with a single measurement setup, *Optica* **4**, 993 (2017).
- [3] A. M. Childs, Universal computation by quantum walk, *Phys. Rev. Lett.* **102**, 180501 (2009).
- [4] E. A. Wollack, A. Y. Cleland, R. G. Gruenke, Z. Wang, P. Arrangoiz-Arriola, and A. H. Safavi-Naeini, Quantum state preparation and tomography of entangled mechanical resonators, *Nature (London)* **604**, 463 (2022).
- [5] Y. Aharonov, L. Davidovich, and N. Zagury, Quantum random walks, *Phys. Rev. A* **48**, 1687 (1993).
- [6] N. B. Lovett, S. Cooper, M. Everitt, M. Trevers, and V. Kendon, Universal quantum computation using the discrete-time quantum walk, *Phys. Rev. A* **81**, 042330 (2010).
- [7] M. Szegedy, Quantum speed-up of Markov chain based algorithms, in *45th Annual IEEE Symposium on Foundations of Computer Science (IEEE, 2004)*, pp. 32–41.
- [8] G. D. Paparo, M. Müller, F. Comellas, and M. A. Martin-Delgado, Quantum Google algorithm, *Eur. Phys. J. Plus* **129**, 150 (2014).
- [9] L. Yan-Mei, C. Han-Wu, L. Zhi-Hao, X. Xi-Ling, and Z. Wan-Ning, Scattering quantum walk search algorithm on star graph, *Acta Phys. Sin.* **64**, 010301 (2015).
- [10] X. L. Xue, H. W. Chen, Z. H. Liu, and B. B. Zhang, Search algorithm of structure anomalies in complete graph based on scattering quantum walk, *Wuli Xuebao/Acta Physica Sinica* **65**, 080302 (2016).
- [11] J. G. Titchener, A. S. Solntsev, and A. A. Sukhorukov, Two-photon tomography using on-chip quantum walks, *Opt. Lett.* **41**, 4079 (2016).
- [12] M. L. Rhodes and T. G. Wong, Quantum walk search on the complete bipartite graph, *Phys. Rev. A* **99**, 032301 (2019).
- [13] G. Martín-Vázquez and J. Rodríguez-Laguna, Optimizing the spatial spread of a quantum walk, *Phys. Rev. A* **102**, 022223 (2020).

- [14] C. Huang, X. Liu, M. Deng, Y. Zhou, and D. Bu, A survey on algorithms for epidemic source identification on complex networks, *Chin. J. Comput.* **41**, 1156 (2018).
- [15] X. Wang, Y. Zhang, K. Lu, X. Wang, and K. Liu, [Detecting multiple information sources based on the quantum walk](#), in *2018 5th International Conference on Systems and Informatics (ICSAI)* (IEEE, 2018).
- [16] S.-L. Peng, H.-J. Wang, H. Peng, X.-B. Zhu, X. Li, J. Han, D. Zhao, and Z.-L. Hu, NLSI: An innovative method to locate epidemic sources on the SEIR propagation model, *Chaos* **33**, 083125 (2023).
- [17] K. Zhu and L. Ying, Information source detection in the sir model: A sample-path-based approach, *IEEE/ACM Trans. Netw.* **24**, 408 (2014).
- [18] N. Antulov-Fantulin, A. Lančić, T. Šmuc, H. Štefančić, and M. Šikić, Identification of patient zero in static and temporal networks: Robustness and limitations, *Phys. Rev. Lett.* **114**, 248701 (2015).
- [19] J. Jiang, S. Wen, S. Yu, Y. Xiang, and W. Zhou, K-center: An approach on the multi-source identification of information diffusion, *IEEE Trans. Inf. Forensics Secur.* **10**, 2616 (2015).
- [20] L. Fu, Z. Shen, W.-X. Wang, Y. Fan, and Z. Di, Multi-source localization on complex networks with limited observers, *Europhys. Lett.* **113**, 18006 (2016).
- [21] D. Shah and T. Zaman, Rumors in a network: Who's the culprit? *IEEE Trans. Inf. Theory* **57**, 5163 (2011).
- [22] P. C. Pinto, P. Thiran, and M. Vetterli, Locating the source of diffusion in large-scale networks, *Phys. Rev. Lett.* **109**, 068702 (2012).
- [23] H.-J. Wang, F.-F. Zhang, and K.-J. Sun, An algorithm for locating propagation source in complex networks, *Phys. Lett. A* **393**, 127184 (2021).
- [24] H.-J. Wang and K.-J. Sun, Locating source of heterogeneous propagation model by universal algorithm, *Europhys. Lett.* **131**, 48001 (2020).
- [25] Z.-L. Hu, X. Han, Y.-C. Lai, and W.-X. Wang, Optimal localization of diffusion sources in complex networks, *R. Soc. Open Sci.* **4**, 170091 (2017).
- [26] W. Hongjue and Z. Fangfeng, Locating sources of complex quantum networks, *New J. Phys.* **24**, 103025 (2022).
- [27] V. Zaburdaev, I. Fouxon, S. Denisov, and E. Barkai, Superdiffusive dispersals impart the geometry of underlying random walks, *Phys. Rev. Lett.* **117**, 270601 (2016).
- [28] T. Schwartz, G. Bartal, S. Fishman, and M. Segev, Transport and Anderson localization in disordered two-dimensional photonic lattices, *Nature (London)* **446**, 52 (2007).
- [29] Y. Lahini, A. Avidan, F. Pozzi, M. Sorel, R. Morandotti, D. N. Christodoulides, and Y. Silberberg, Anderson localization and nonlinearity in one-dimensional disordered photonic lattices, *Phys. Rev. Lett.* **100**, 013906 (2008).
- [30] F. Caruso, A. Crespi, A. G. Ciriolo, F. Sciarrino, and R. Osellame, Fast escape of a quantum walker from an integrated photonic maze, *Nat. Commun.* **7**, 11682 (2016).
- [31] D. L. Donoho, Compressed sensing, *IEEE Trans. Inf. Theory* **52**, 1289 (2006).
- [32] Y. C. Eldar and G. Kutyniok, *Compressed Sensing: Theory and Applications* (Cambridge University Press, Cambridge, UK, 2012).
- [33] E. Candès and J. Romberg, Recovery of sparse signals via convex programming, Caltech, Oct (2005), www.acm.caltech.edu/l1magic/downloads/l1magic.pdf.
- [34] E. Candes and T. Tao, The Dantzig selector: Statistical estimation when p is much larger than n , *Ann. Statist.* **35**, 2313 (2007).
- [35] R. Albert and A.-L. Barabási, Statistical mechanics of complex networks, *Rev. Mod. Phys.* **74**, 47 (2002).
- [36] A.-L. Barabási and R. Albert, Emergence of scaling in random networks, *Science* **286**, 509 (1999).
- [37] D. J. Watts and S. H. Strogatz, Collective dynamics of 'small-world' networks, *Nature (London)* **393**, 440 (1998).
- [38] G. Palla, I. Derényi, I. Farkas, and T. Vicsek, Uncovering the overlapping community structure of complex networks in nature and society, *Nature (London)* **435**, 814 (2005).
- [39] S. Fortunato, Community detection in graphs, *Phys. Rep.* **486**, 75 (2010).
- [40] D. Lusseau, K. Schneider, O. J. Boisseau, P. Haase, E. Slooten, and S. M. Dawson, The bottlenose dolphin community of doubtful sound features a large proportion of long-lasting associations, *Behav. Ecol. Sociobiol.* **54**, 396 (2003).
- [41] R. Milo, S. Itzkovitz, N. Kashtan, R. Levitt, S. Shen-Orr, I. Ayzenshtat, M. Sheffer, and U. Alon, Superfamilies of evolved and designed networks, *Science* **303**, 1538 (2004).
- [42] H. Wang, An universal algorithm for source location in complex networks, *Phys. A (Amsterdam, Neth.)* **514**, 620 (2019).